2015 NETL Crossingcutting Research Review Meeting, Pittsburgh, PA, April 27-30, 2015

Novel Functional Graded Thermal Barrier Coatings in Coal-fired Power Plant Turbines

Jing Zhang
Department of Mechanical Engineering
Indiana University-Purdue University Indianapolis

Grant No.: DOE DE-FE0008868
Program Manager: Richard Dunst

IUPUI

INDIANA UNIVERSITY
PURDUE UNIVERSITY
INDIANAPOLIS

Acknowledgement

- Subcontract: James Knapp (Praxair Surface Technologies)
- Collaborators: Li Li, Don Lemen (Praxair Surface Technologies)
- Yeon-Gil Jung (Changwon National University)
- Yang Ren, Jiangang Sun (Argonne National Laboratory)
- Changdong Wei (OSU), Bin Hu (Dartmouth)
- Ph.D. graduate students: Xingye Guo, Yi Zhang

Outline

- Introduction
- Coating fabrications
- Single ceramic layer (SCL) architecture
- Double ceramic layer (DCL) architecture
- Characterization of physical and mechanical properties
- Microstructure and composition
- Porosity and hardness
- Bond strength test
- Erosion test
- Characterization of thermal properties
- Thermal conductivity and specific heat measurements
- Jet engine thermal shock tests
- Thermal gradient mechanical fatigue tests
- Summary and future work

Limitation of yttria stabilized zirconia

- Zirconia partially stabilized with 7 wt% yttria (7YSZ) is the current state-of-the-art thermal barrier coating material.

- However, at temperatures higher than 1200 ^{o}C, YSZ layers are prone to **sintering**, which increases thermal conductivity and makes them less effective.

- The sintered and densified coatings can also **reduce thermal stress and strain tolerance**, which can reduce the coating's durability significantly.

Motivation and objective

- To further increase the operating temperature of turbine engines, alternative TBC materials with lower thermal conductivity, higher operating temperatures and better sintering resistance are required.
- The objective of the project is to develop a novel lanthanum zirconate based multi-layer thermal barrier coating system.
- The ultimate goal is to develop a manufacturing process to produce pyrochlore oxide based coating with improved high-temperature properties.

Pyrochlore - $A_2B_2O_7$

Pyrochlore-type rare earth zirconium oxides ($Re_2Zr_2O_7$,Re = rare earth) are promising candidates for thermal barrier coatings, high-permittivity dielectrics, potential solid electrolytes in high-temperature fuel cells, and immobilization hosts of actinides in nuclear waste.

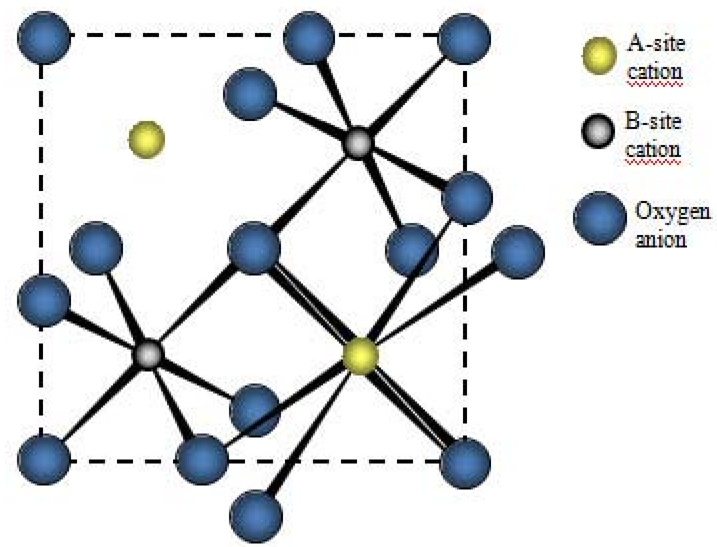

Pyrochlore crystal structure: $A_2B_2O_7$. A and B are metals incorporated into the structure in various combinations. (credit: NETL)

Why $La_2Zr_2O_7$?

Compared with YSZ, $La_2Zr_2O_7$ has

- Higher temperature phase stability. No phase transformation
- Lower sintering rate at elevated temperature
- Lower thermal conductivity
- Lower CTE

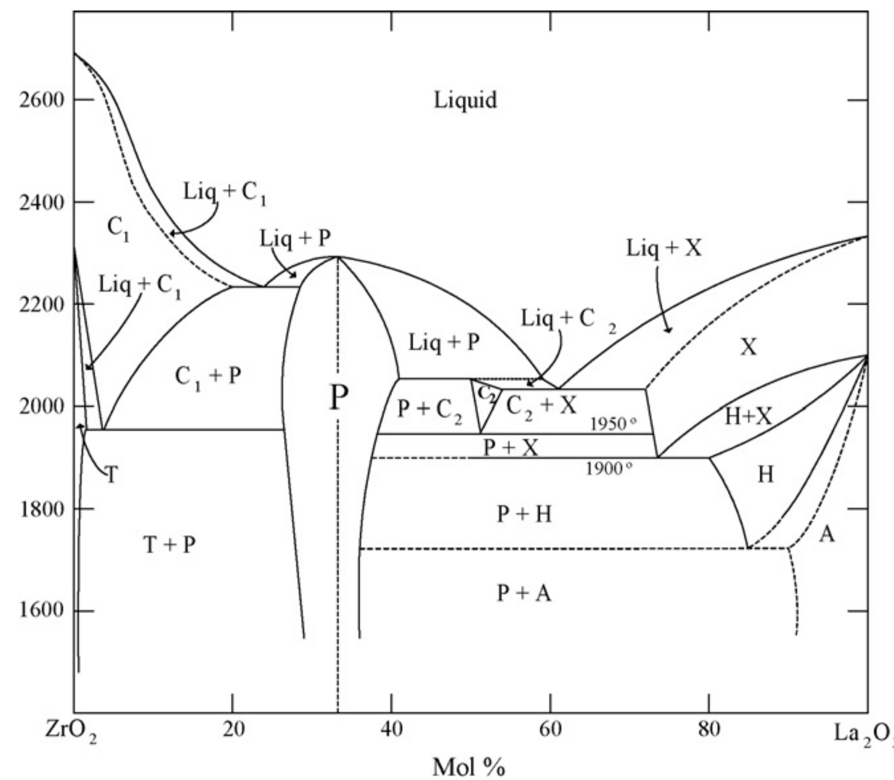

Phase diagram of La_2O_3–ZrO_2

$La_2Zr_2O_7$ vs. YSZ

Materials property	8YSZ	$La_2Zr_2O_7$
Melting Point (^oC)	2680	2300
Maximum Operating Temperature (^oC)	1200	>1300
Thermal Conductivity (W/m-K) (@ 800^oC)	2.12	1.6
Coefficient of Thermal Expansion ($x10^{-6}$/K) (@1000 ^oC)	11.0	8.9-9.1
Density (g/cm^3)	6.07	6.00
Specific heat (J/g-K) (@1000 ^oC)	0.64	0.54

Layered coating architecture

- The coefficient of thermal expansion of $La_2Zr_2O_7$ (10×10^{-6} /°C) is lower than those of both substrate and bondcoat (about 15×10^{-6}/°C @ 1000 °C). As a result, the thermal cycling properties may be a concern
- The layered topcoat architecture is believed to be a feasible solution to improve thermal strain tolerance
- In this work, we develop a multi-layer, functionally graded, pyrochlore oxide based TBC system

$La_2Zr_2O_7$ spray powder morphology

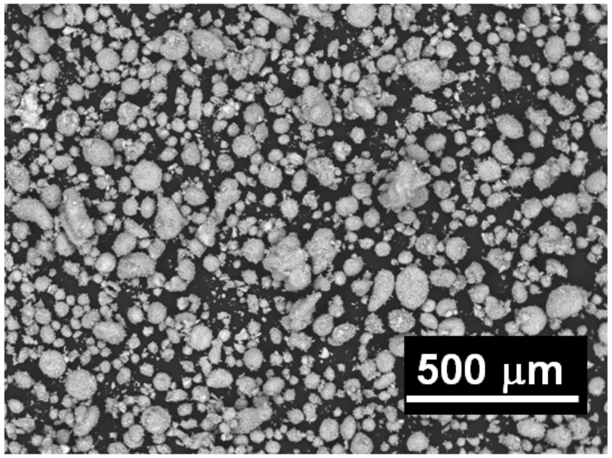

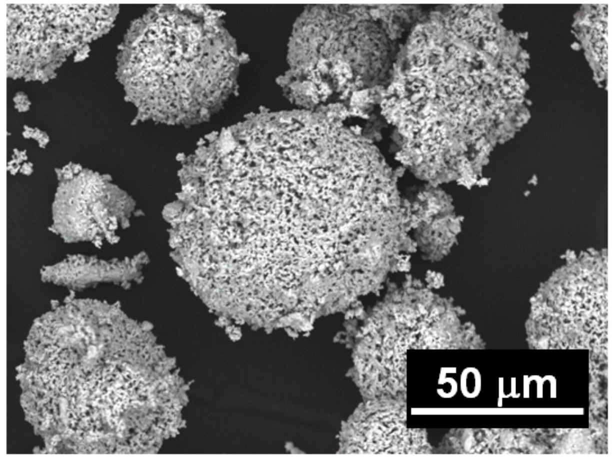

<u>Powder surface morphology</u>

- Spherical shape with a rough surface
- Good flowability and high density
- Particle size between 30 ~ 100 μm

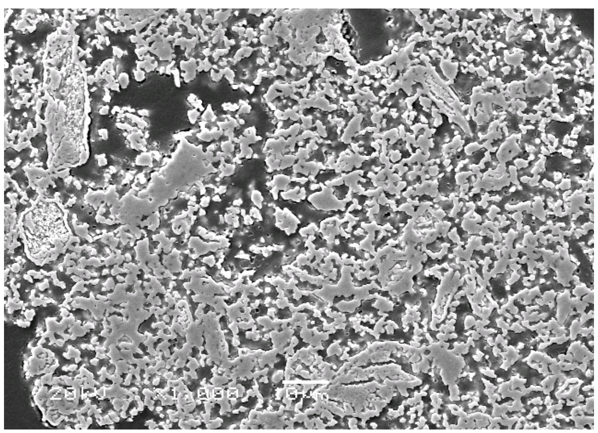

+ 125 um

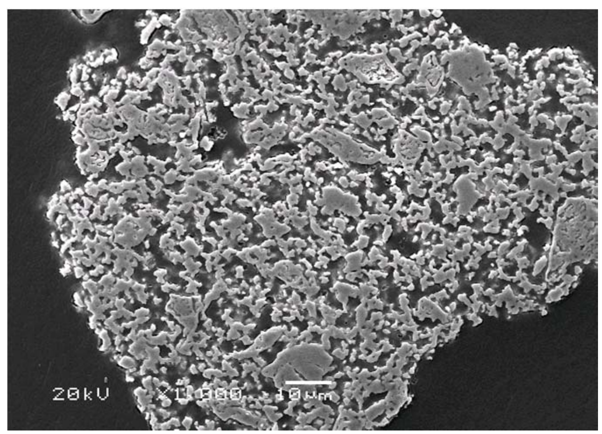

- 125 um

<u>Powder cross-section</u>

- Porous interior

TEM image of $La_2Zr_2O_7$

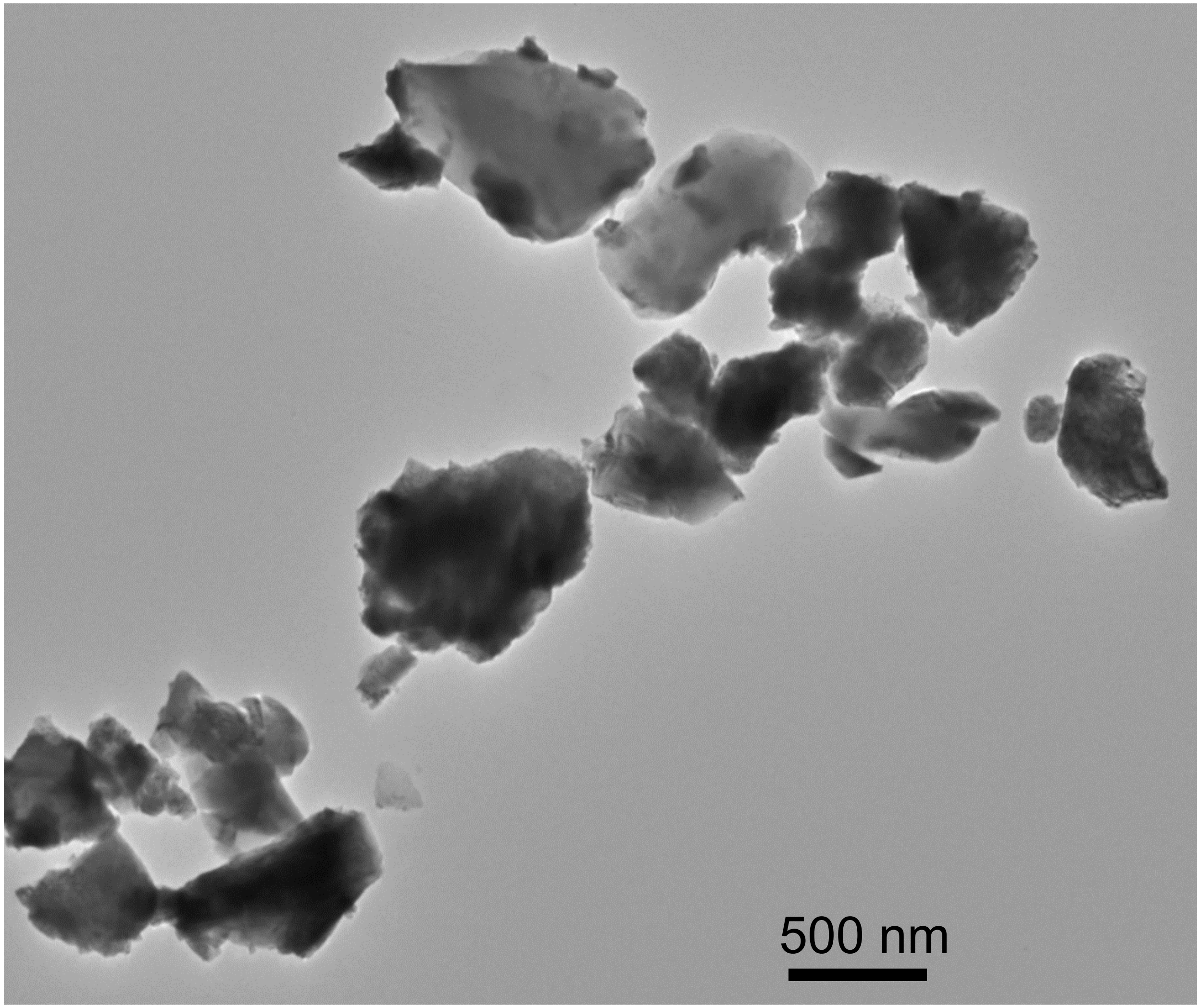

credit: Bin Hu @ Dartmouth

$La_2Zr_2O_7$ powder XRD analysis

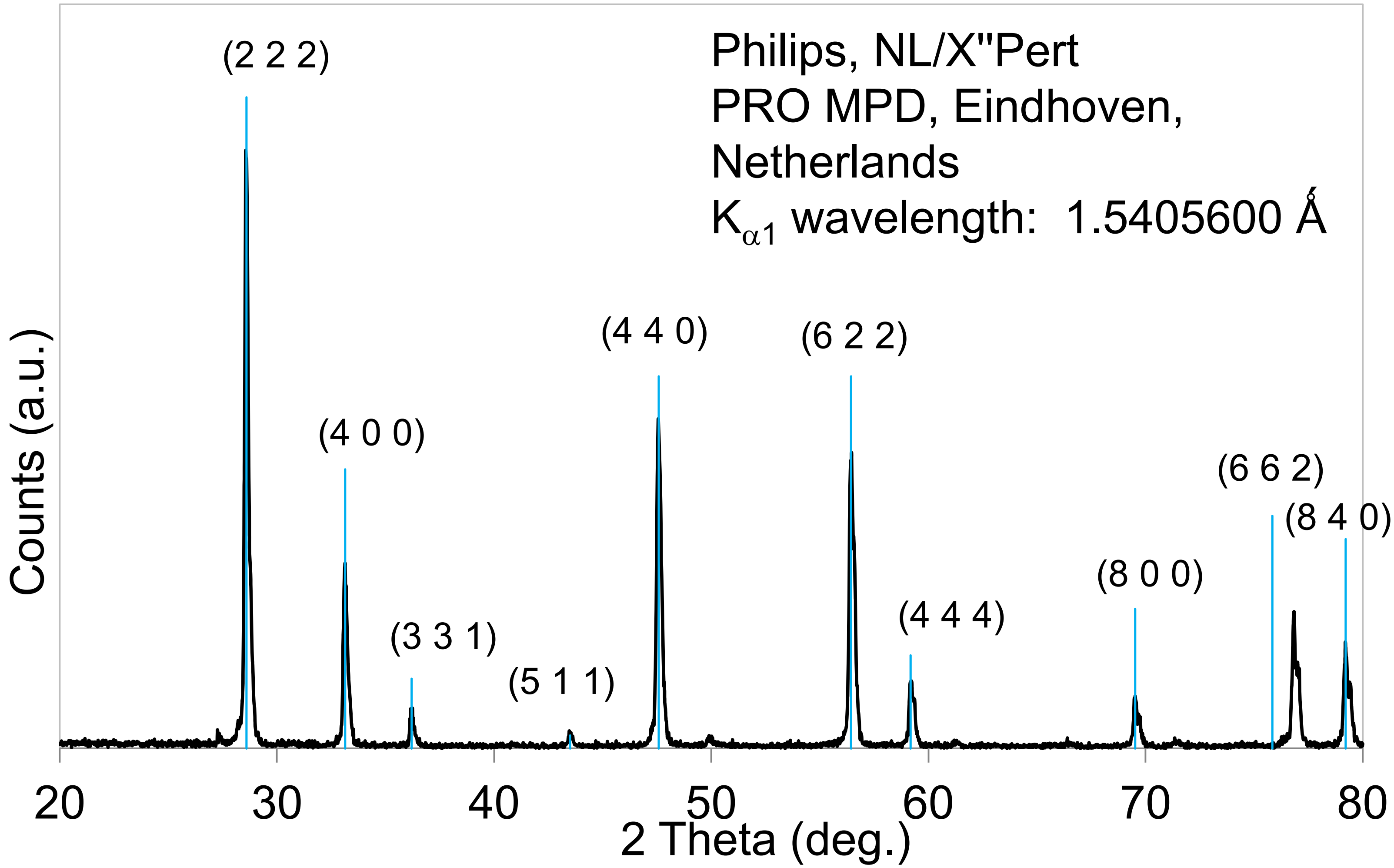

XRD data show that the powder composition is $La_2Zr_2O_7$

Synchrotron XRD

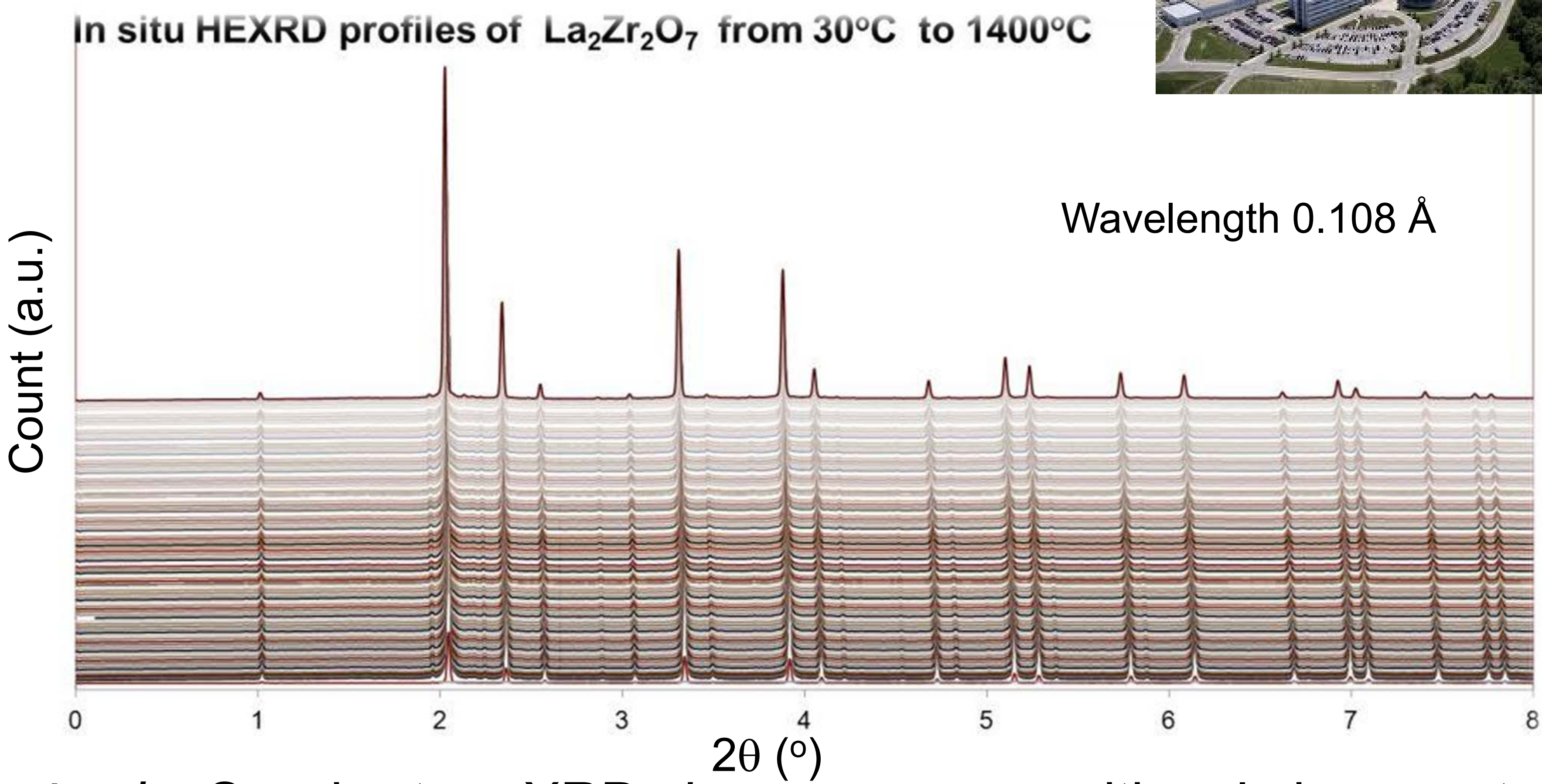

In situ Synchrotron XRD shows no compositional change at high temperatures

credit: Yang Ren @ ANL

Coating fabrication using APS

- $La_2Zr_2O_7$ coatings were deposited using air plasma spray (APS) technique by a Praxair patented plasma spray torch.
- Haynes 188 superalloy was used as the substrate.

Haynes 188	Co	Ni	Cr	W	Si	C	La	Fe	Mn
(w%)	39	22	22	14	0.35	0.10	0.03	3	1.25

- The bond coat is Ni-based intermetallic LN-65 using APS, with a thickness of 228 μm

LN-65	Ni	Cr	Al	Y	O
(w%)	67.3	21.12	9.94	1.02	0.19

- Controlled spray parameters:
- Powder feed ratio
- Torch current
- Torch gas (Argon), Carrier gas (Argon), Shield gas (Argon), Secondary gas (Hydrogen)
- Standoff distance
- Sample rig surface rotation speed (RPM and surface speed)

Outline

- Introduction
- Coating fabrications
- Single ceramic layer (SCL) architecture – dense coating
- Double ceramic layer (DCL) architecture
- Characterization of physical and mechanical properties
- Microstructure
- Hardness and Young's modulus
- Bond strength test
- Erosion test
- Characterization of thermal properties
- Thermal properties
- Jet engine thermal shock tests
- Thermal gradient mechanical fatigue tests
- Summary and future work

Cross sectional view of dense coating

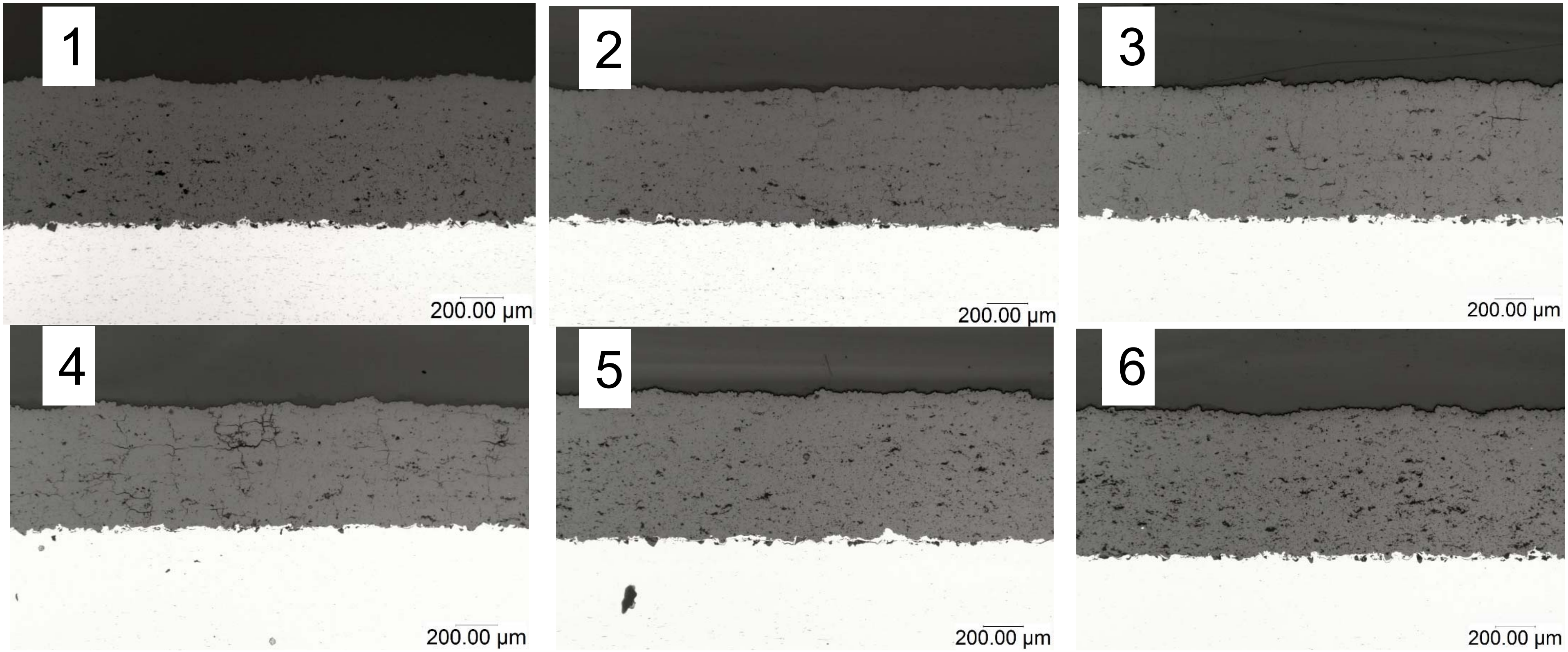

Processing parameters (powder feed rate, surface speed, current, stand off) were varied to control the porosity.

Nanoindentation Young's modulus vs. displacement

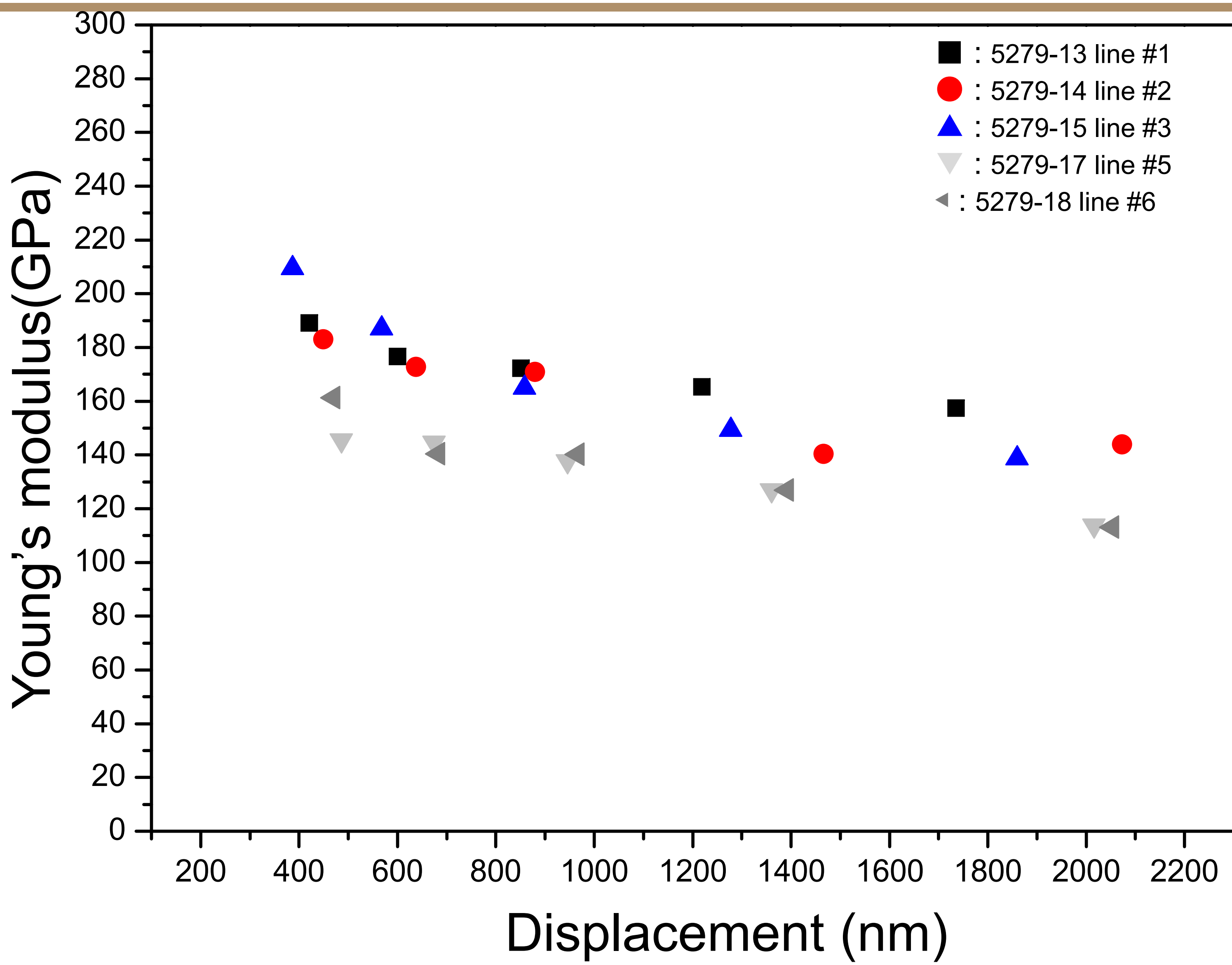

Nanoindentation Young's modulus

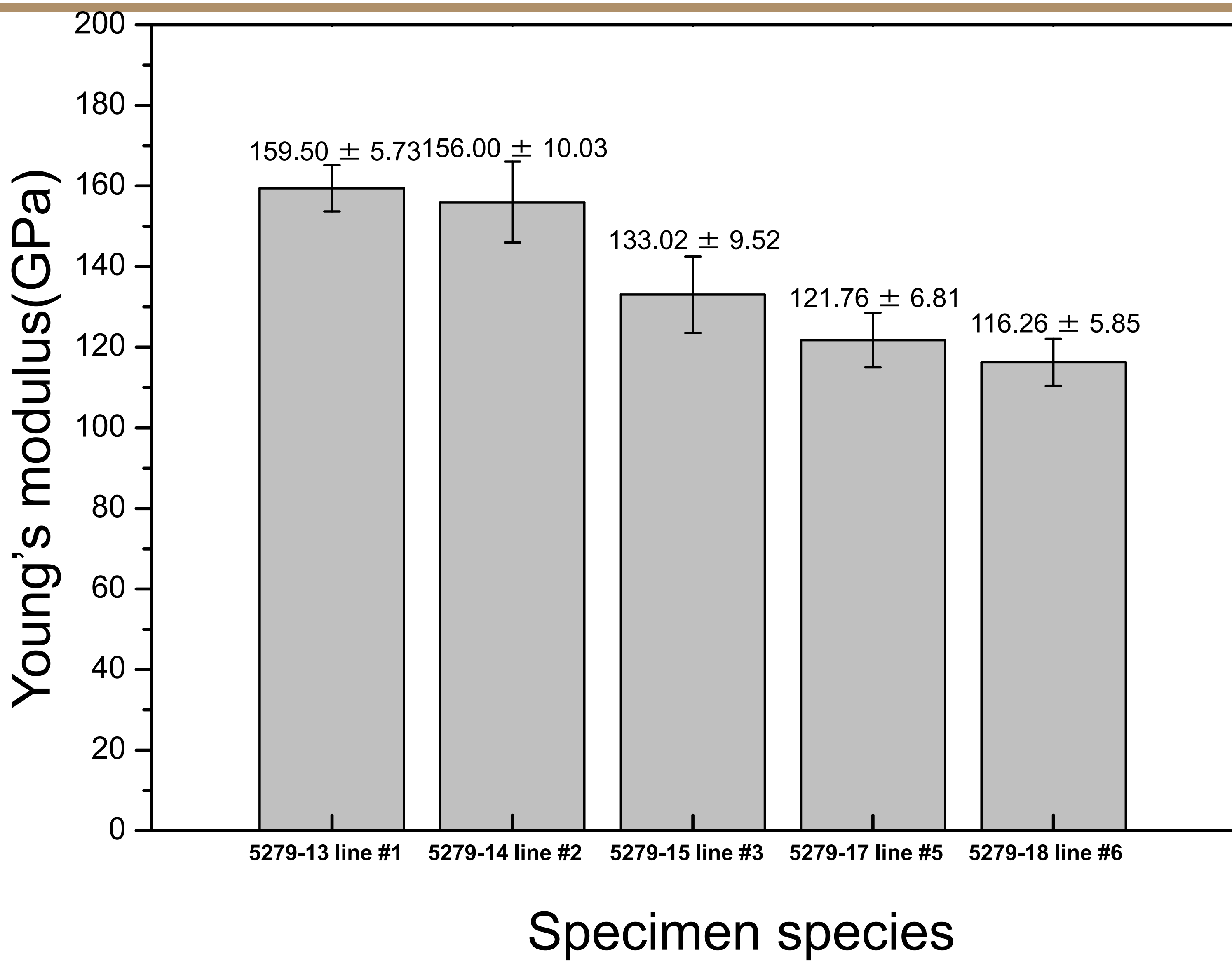

Nanoindentation hardness

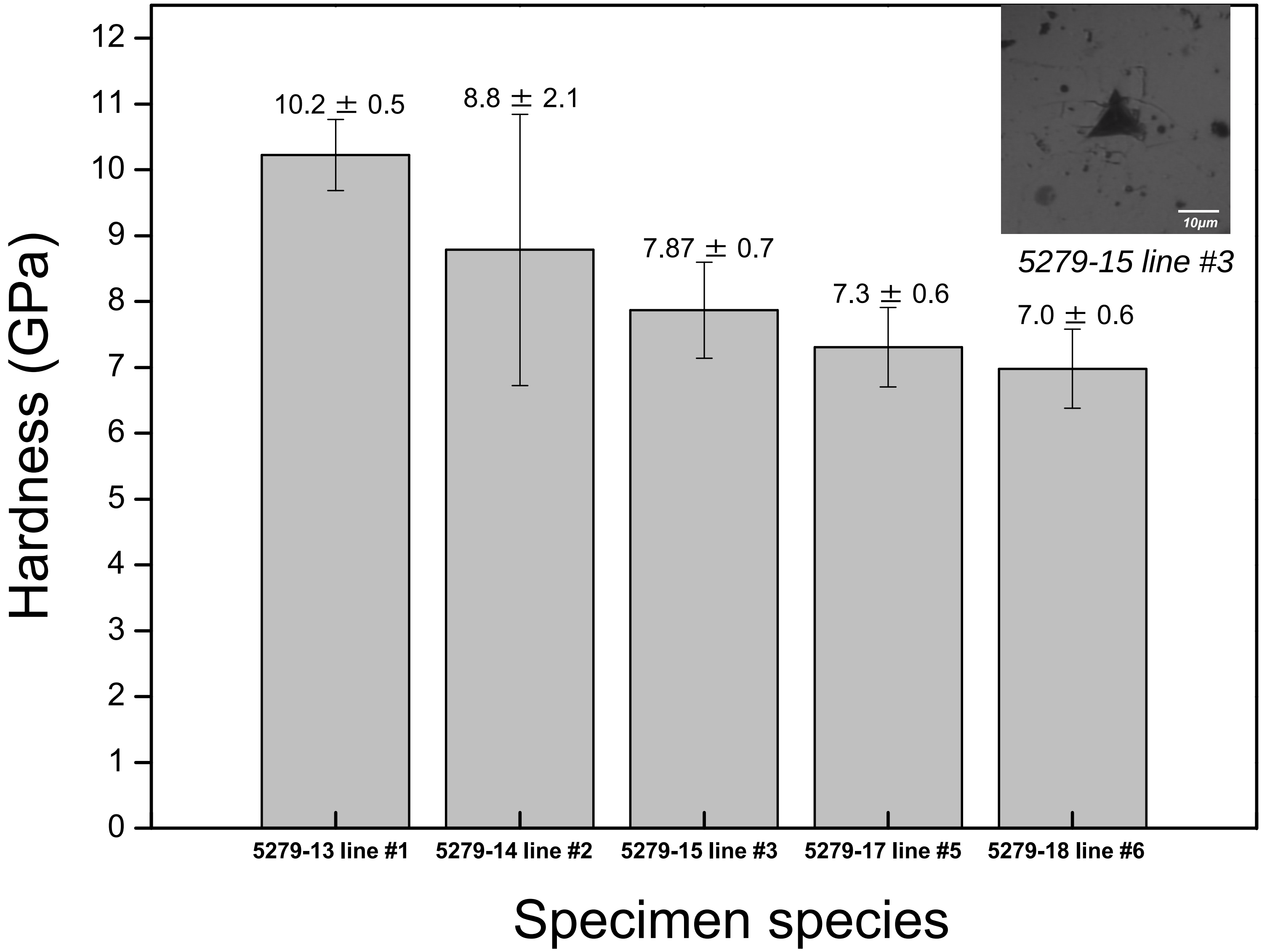

Vicker's indentation hardness

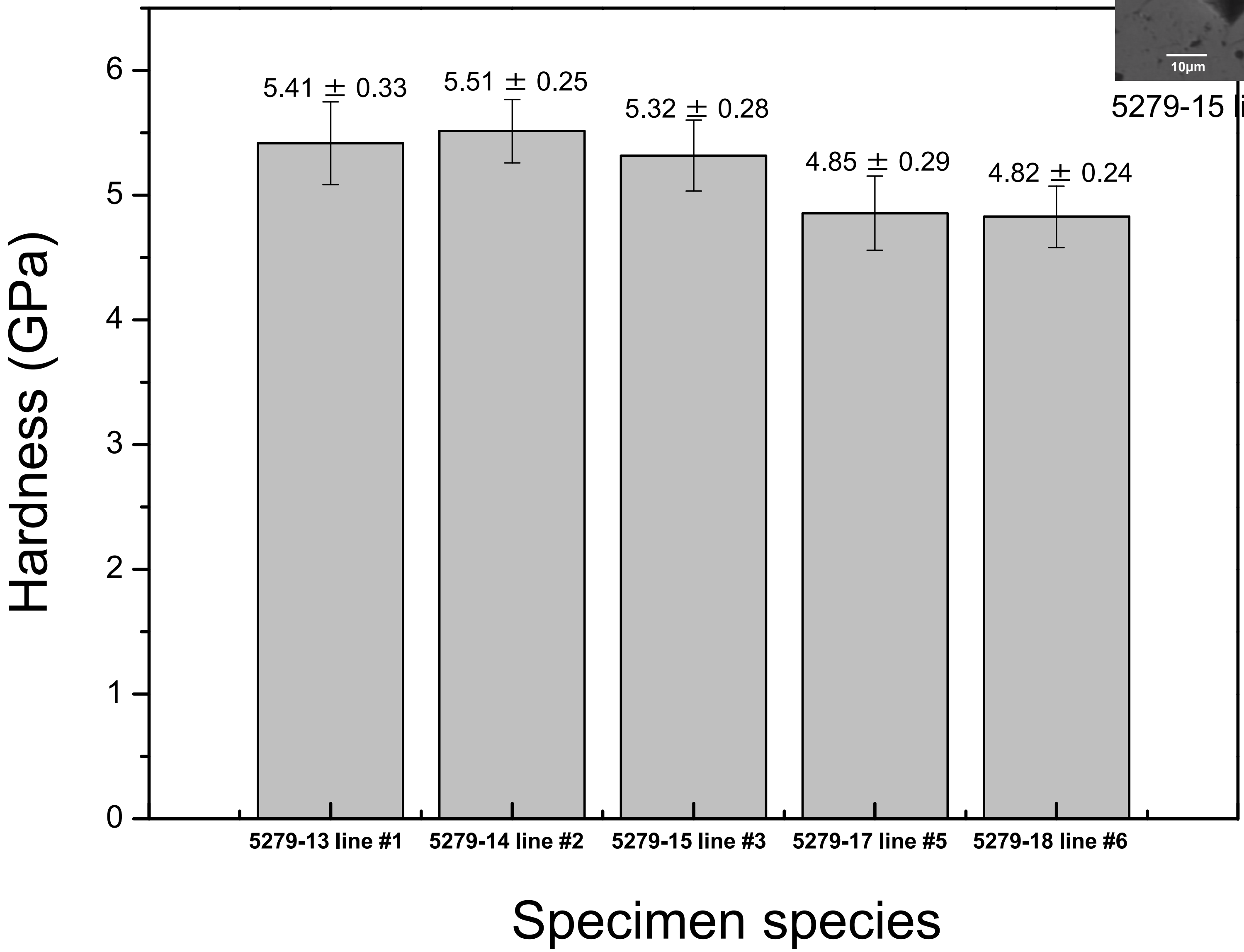

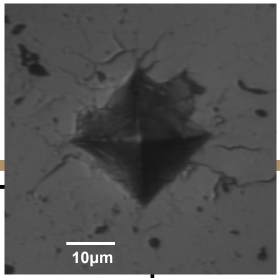

5279-15 line #3

Rockwell's indentation hardness

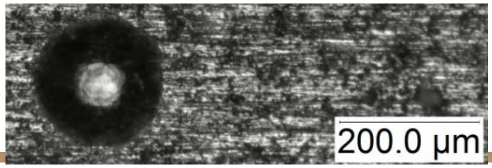

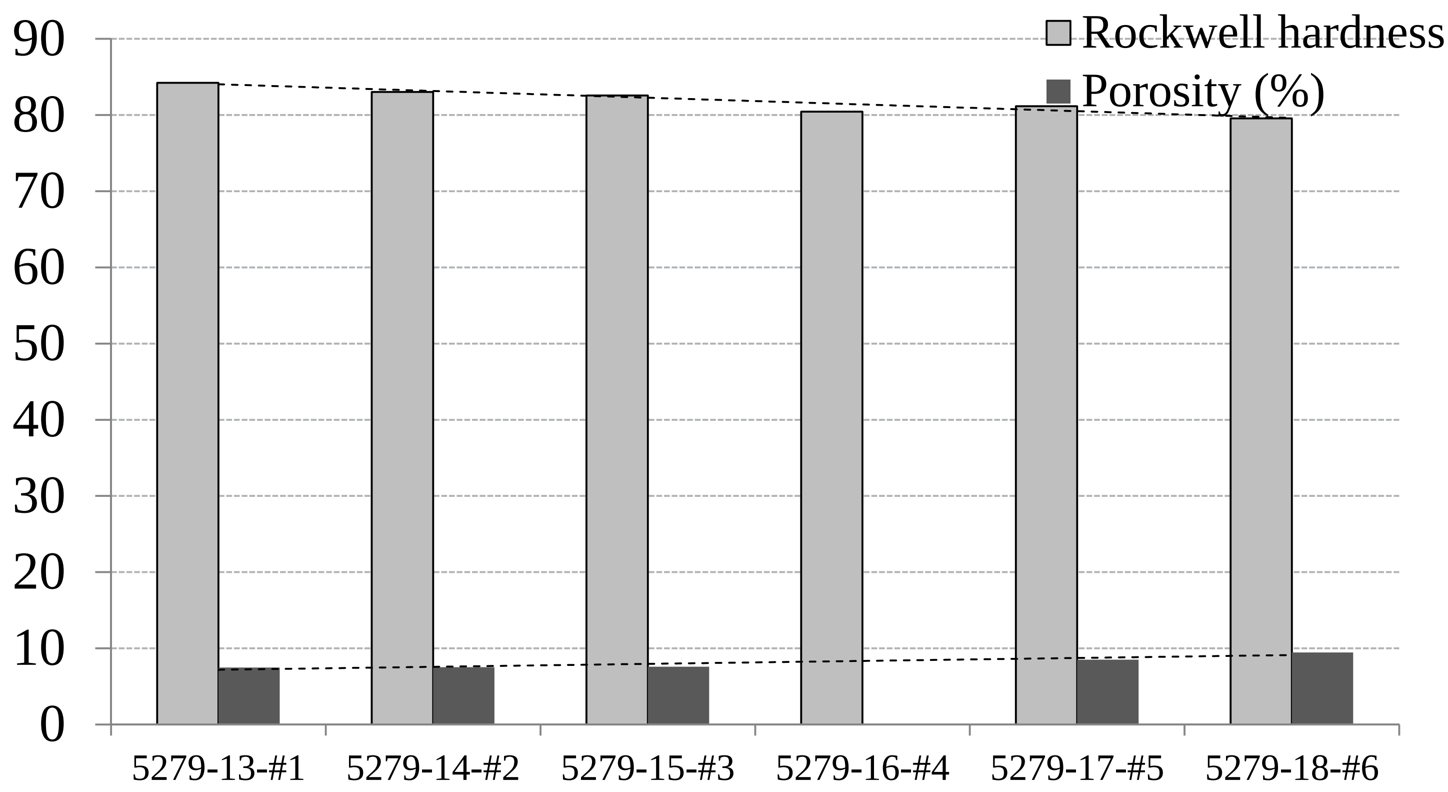

- Low density coatings with porosity between 7~10 % were achieved.
- Porosity and hardness can be tuned via changing processing conditions
- Powder feed rate↑ or current↓ → porosity↑ → hardness↓
  [Hardness = 1.99 × (100-porosity) -100]

Outline

- Introduction
- Coating fabrications
- Single ceramic layer (SCL) architecture – porous coating
- Double ceramic layer (DCL) architecture
- Characterization of physical and mechanical properties
- Microstructure and composition
- Porosity and hardness
- Bond strength test
- Erosion test
- Characterization of thermal properties
- Thermal properties
- Jet engine thermal shock tests
- Thermal gradient mechanical fatigue tests
- Summary and future work

Cross sections of SCL $La_2Zr_2O_7$ coatings

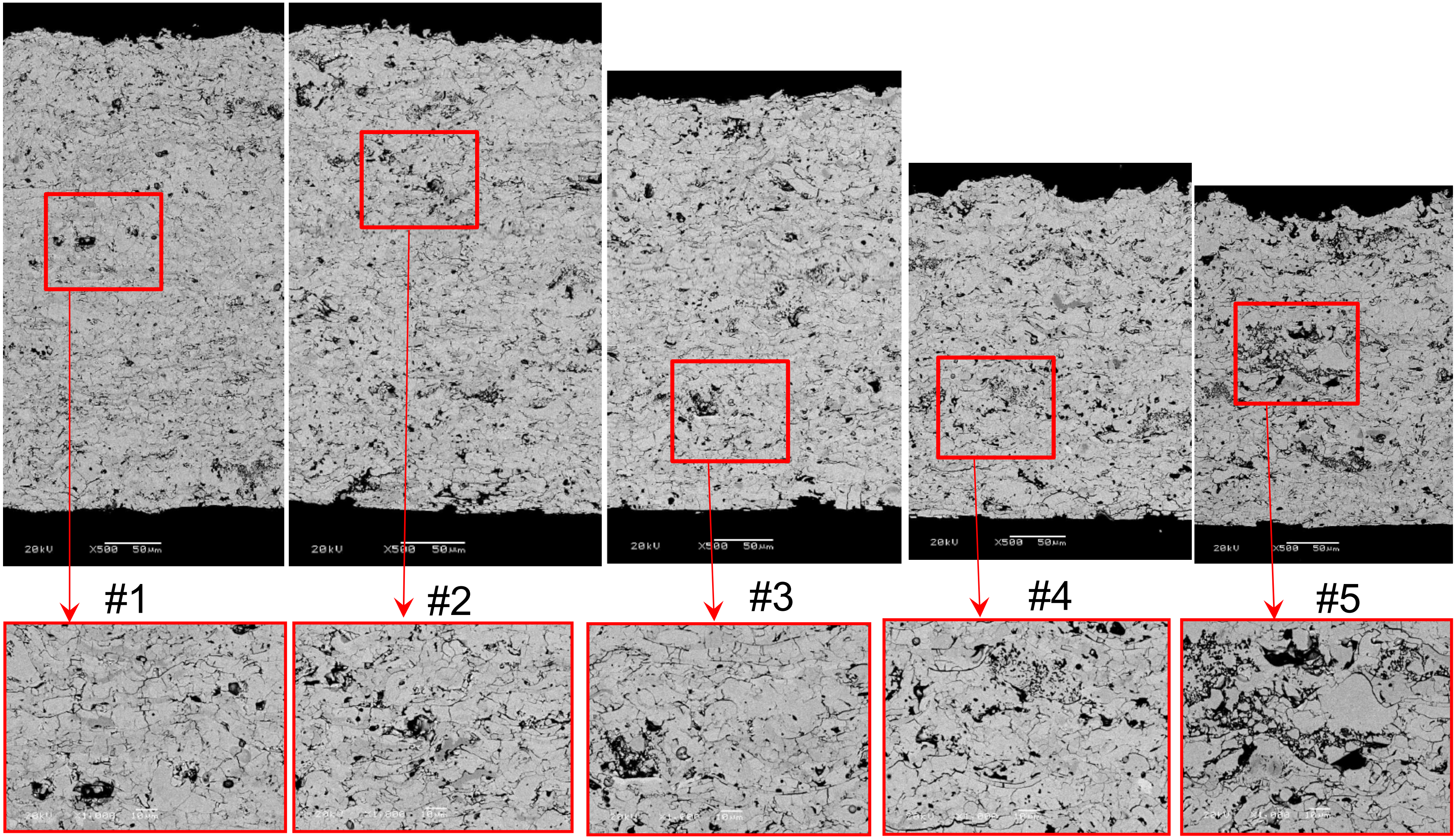

Vickers hardness indentation

#1 #2 #3 #4 #5

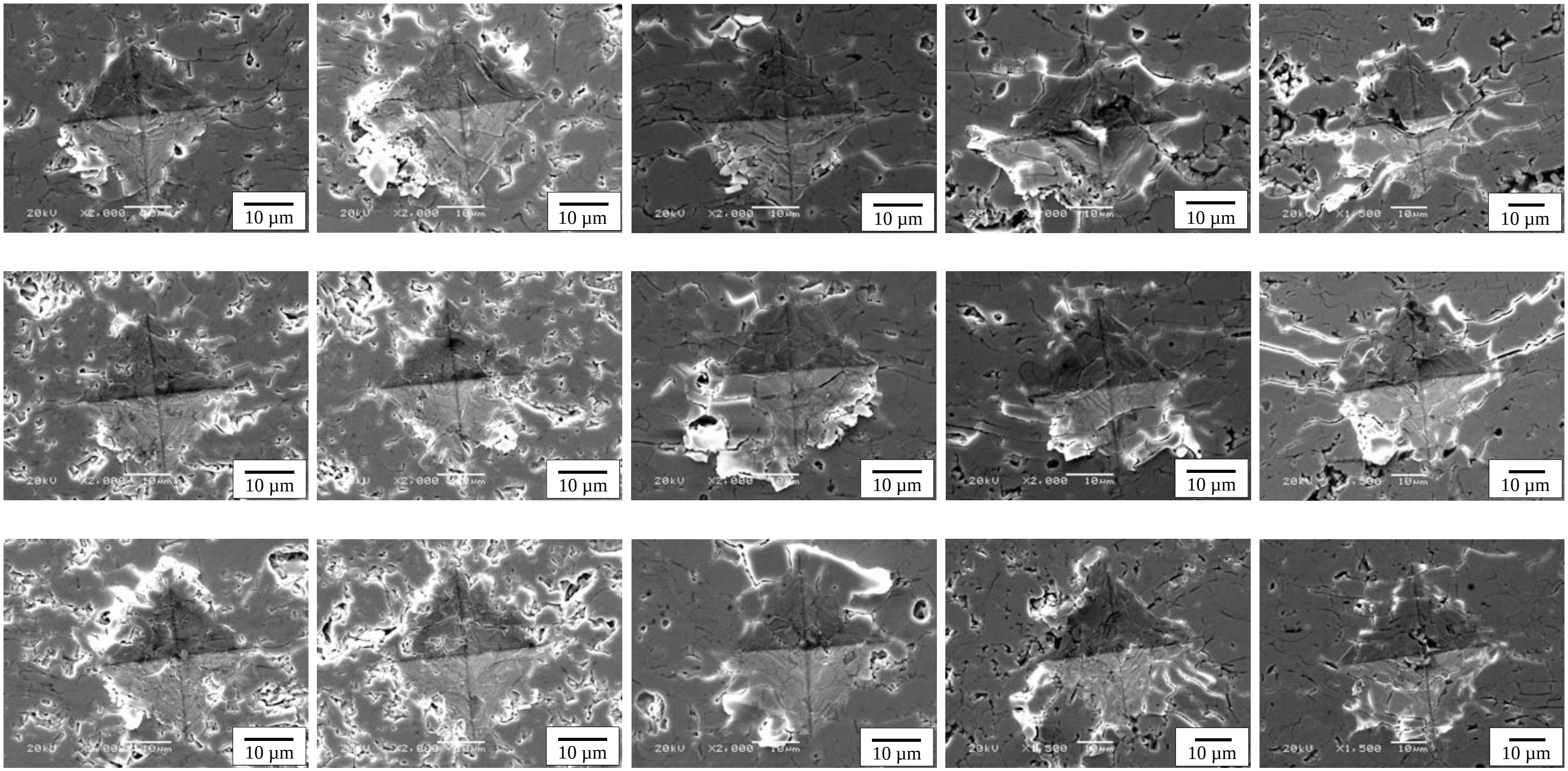

Nanoindentation

#3 #4 #5

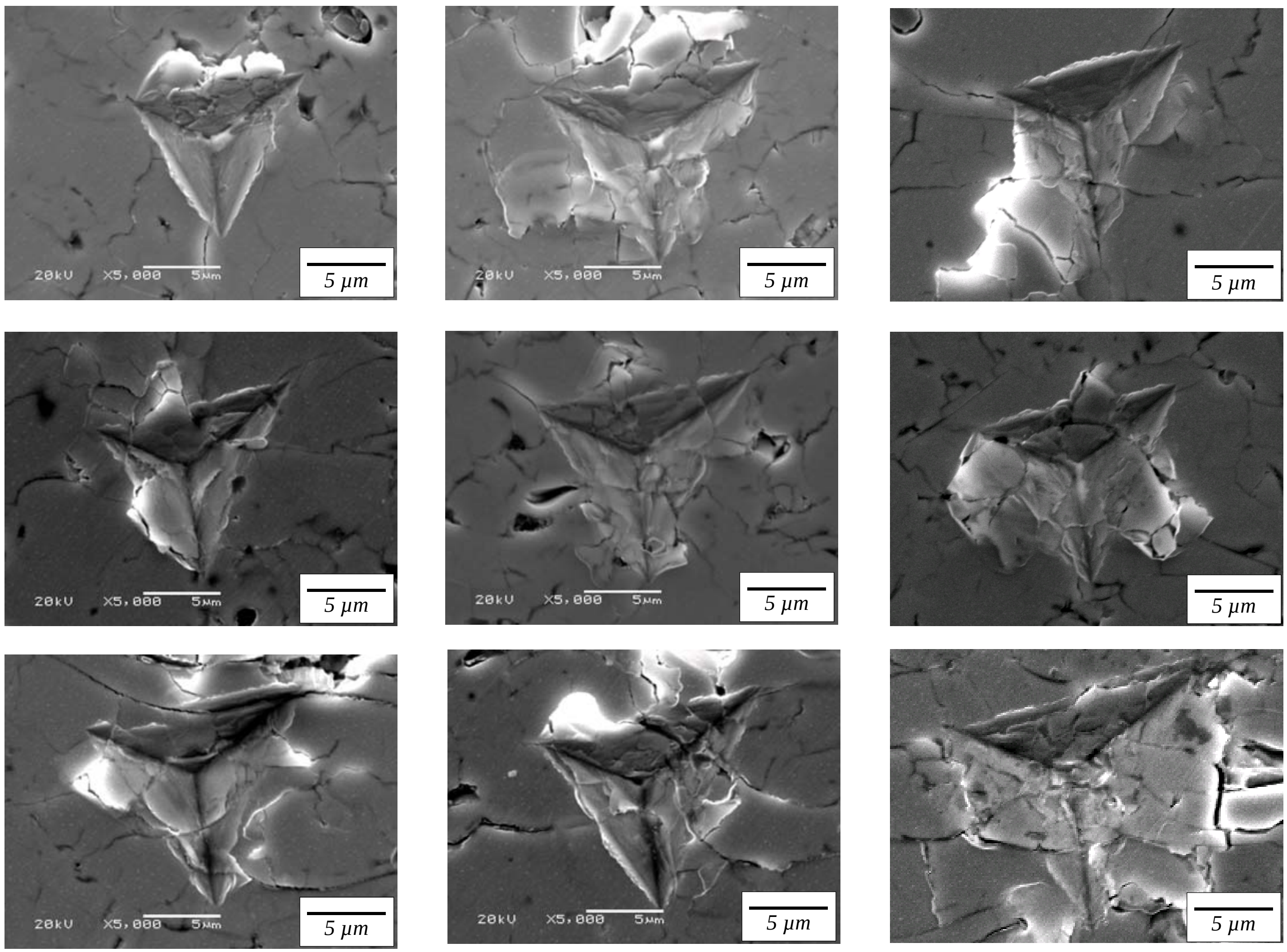

Vickers indentation hardness

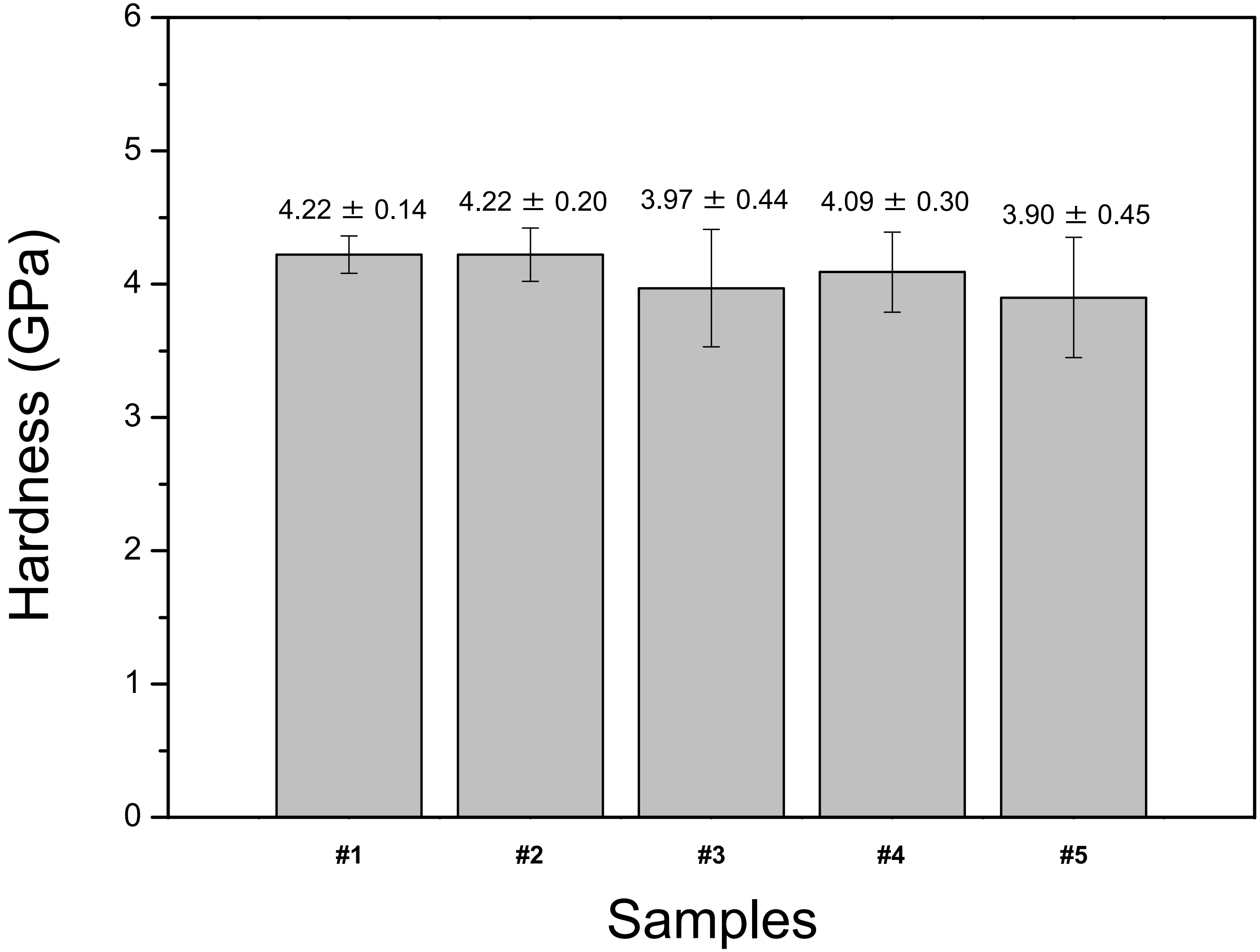

Nano indentation Young's modulus vs. displacement

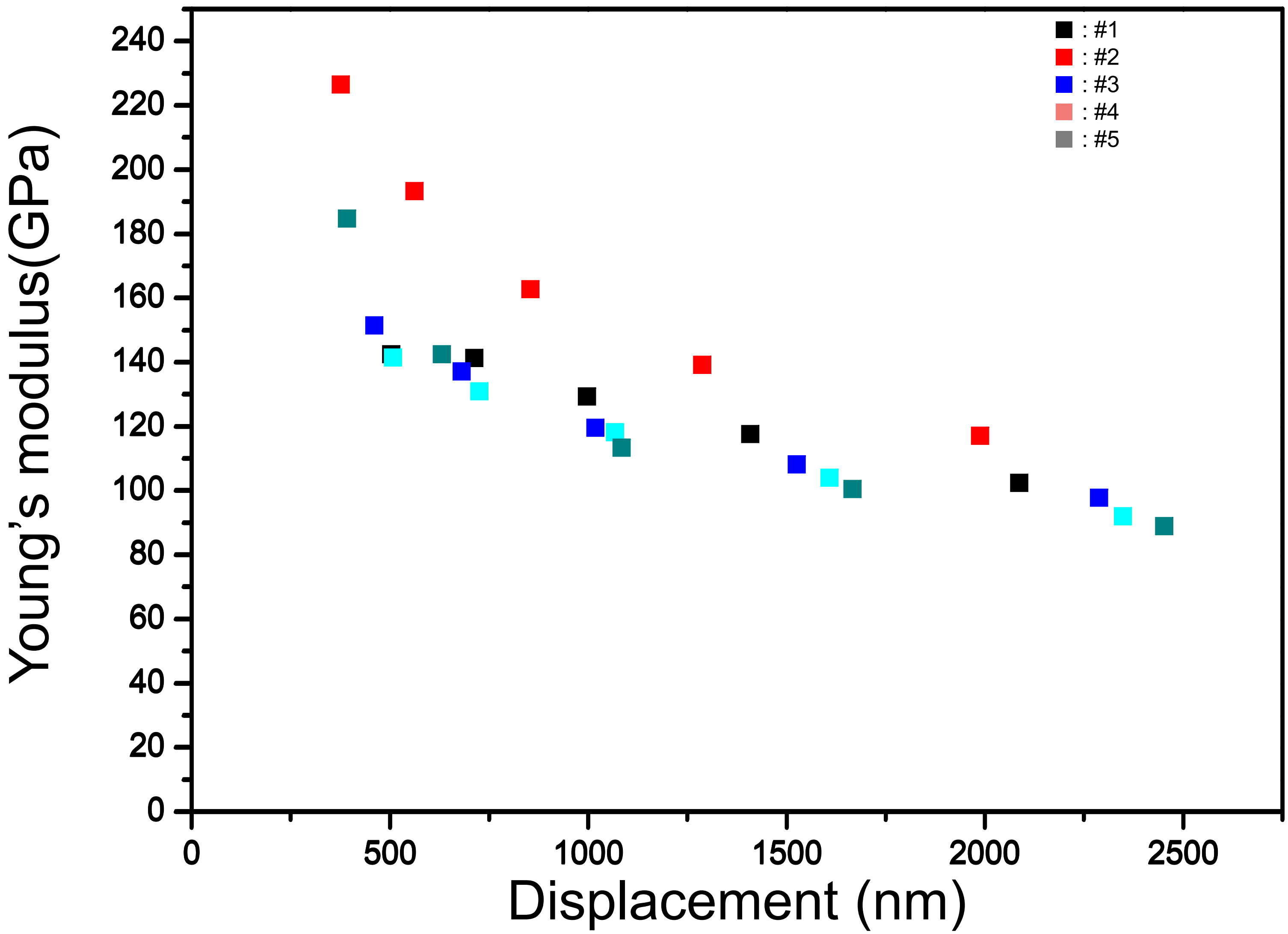

Nanoindentation Young's modulus

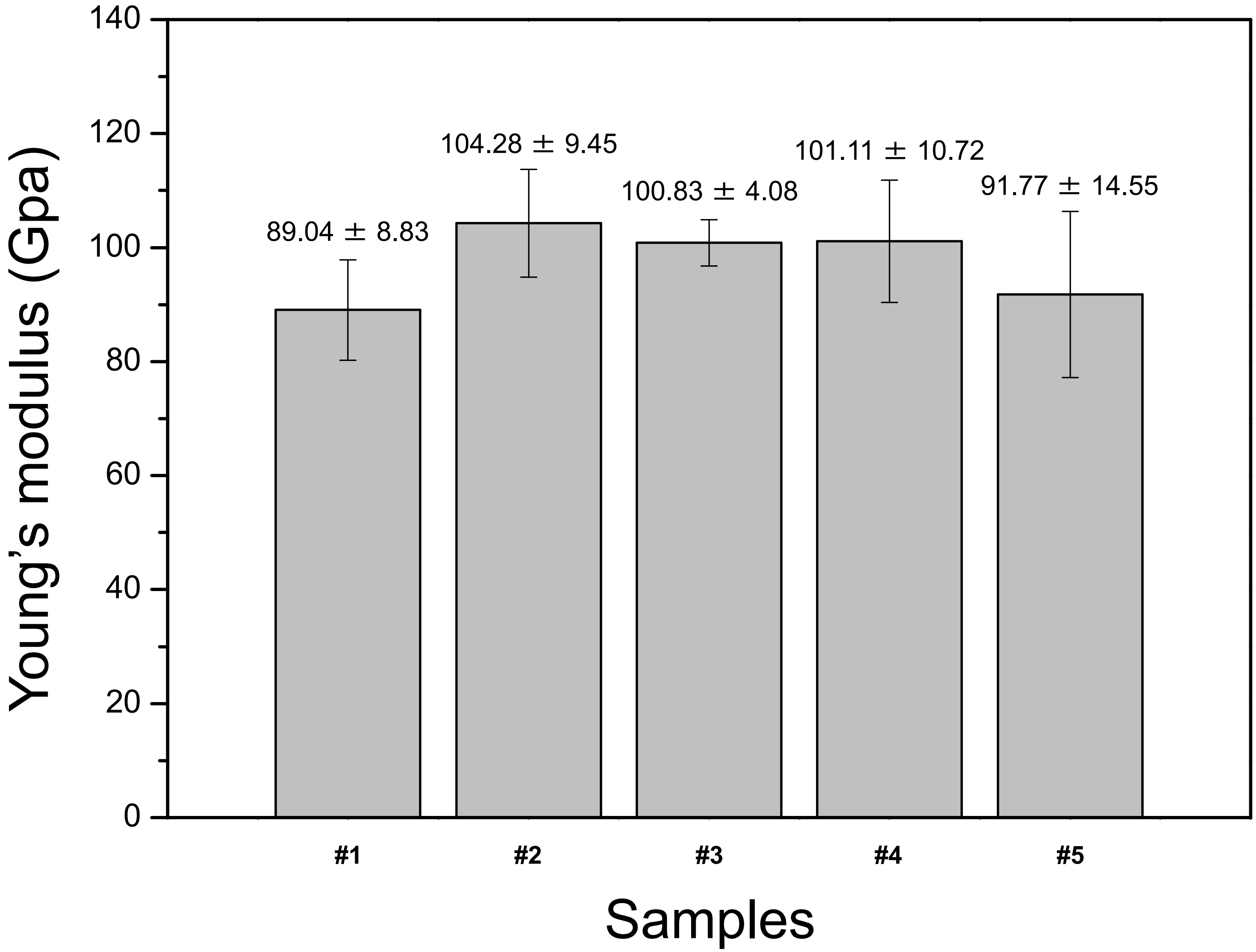

Nanoindentation hardness

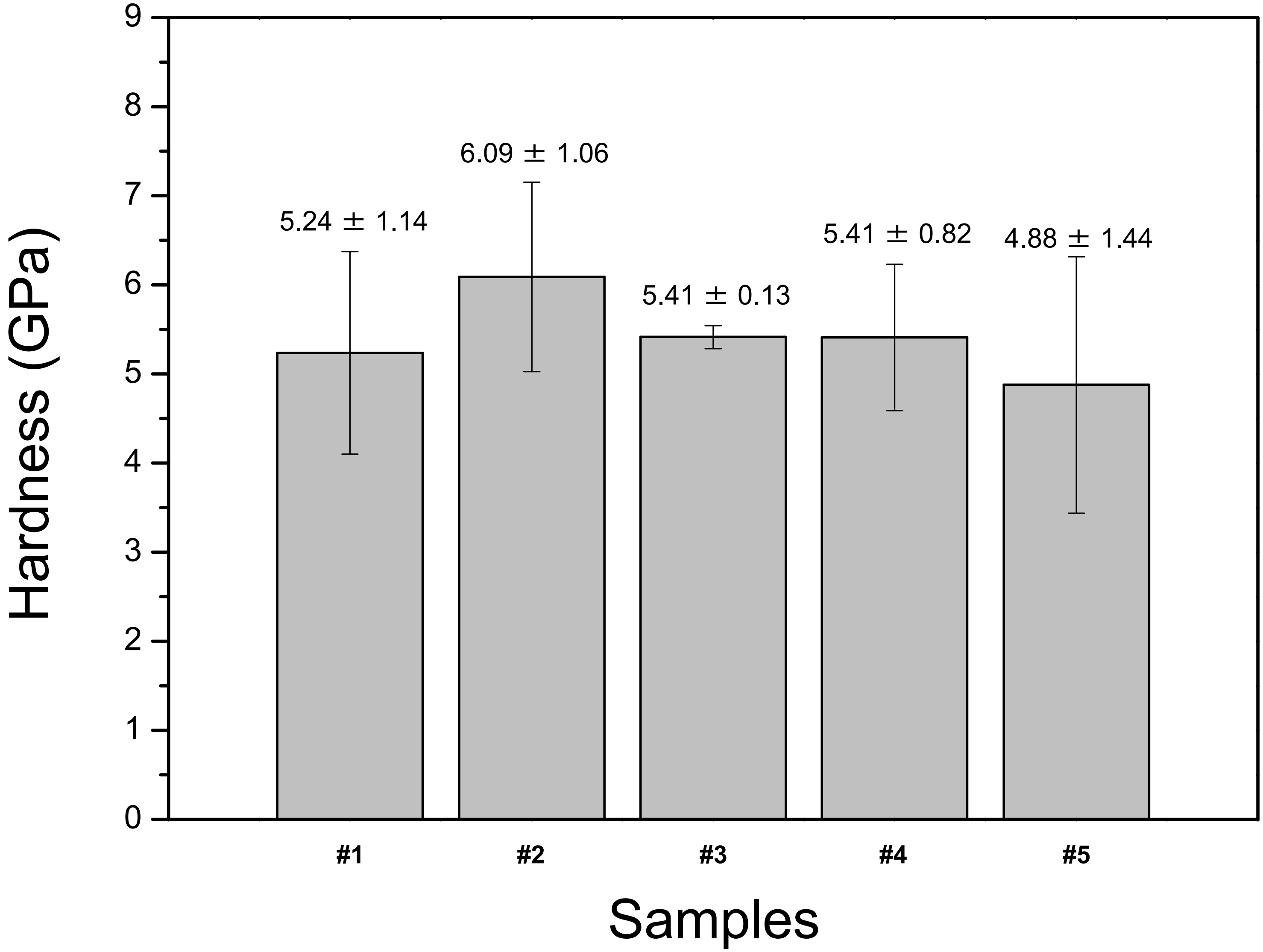

Porosity of low density SCL coating

Line #	Density (g/cm^3)	Porosity (%)
7	5.3182	11.36
8	5.2587	12.36
9	5.2584	12.36
10	5.2917	11.81
11	5.2614	12.31
12	5.0089	16.52

Low density coatings with porosity between 11~17% were achieved.

Outline

- Introduction
- Coating fabrications
- Single ceramic layer (SCL) architecture
- Double ceramic layer (DCL) architecture
- Characterization of physical and mechanical properties
- Microstructure and composition
- Porosity and hardness
- Bond strength test
- Erosion test
- Characterization of thermal properties
- Thermal properties
- Jet engine thermal shock tests
- Thermal gradient mechanical fatigue tests
- Summary and future work

Double ceramic layer (DCL) architectures

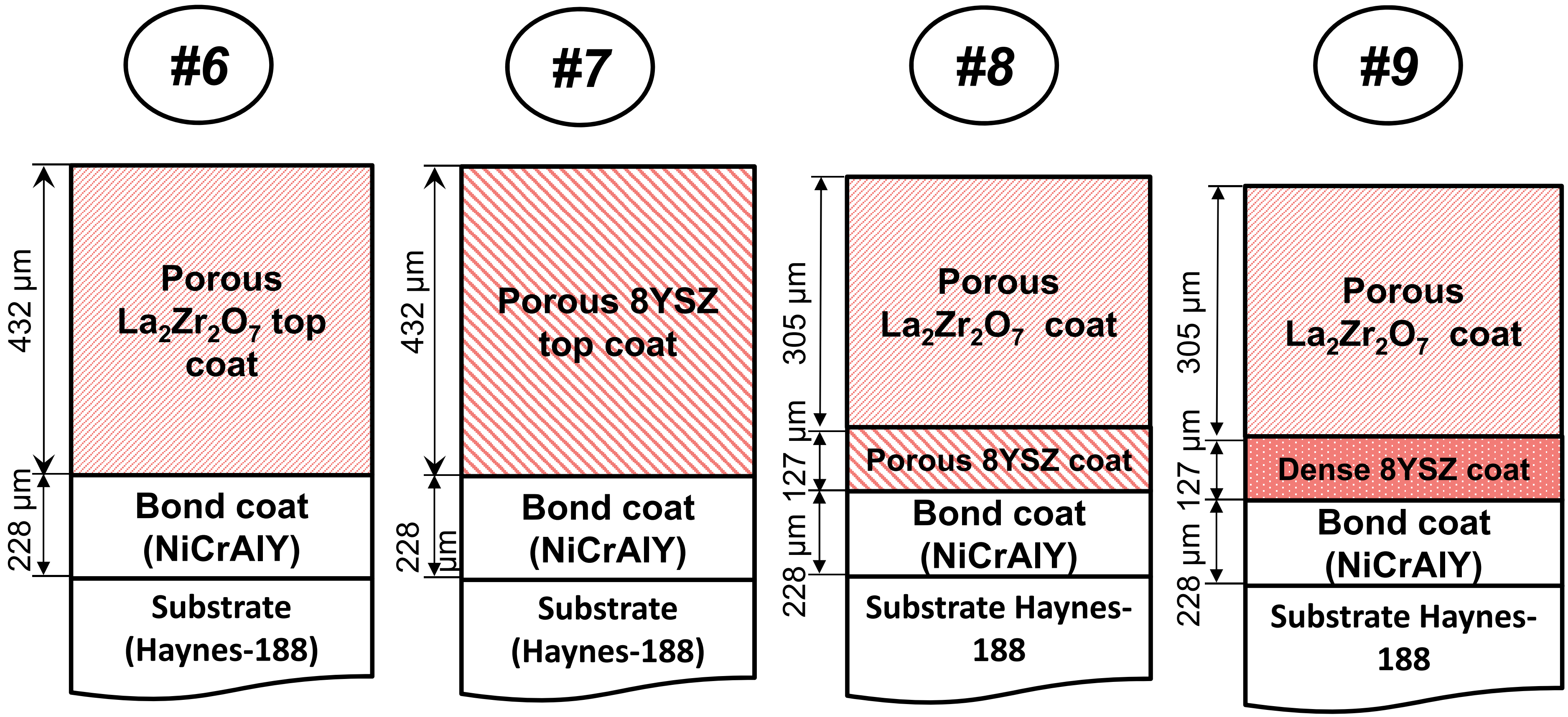

Interfaces of DCL coatings

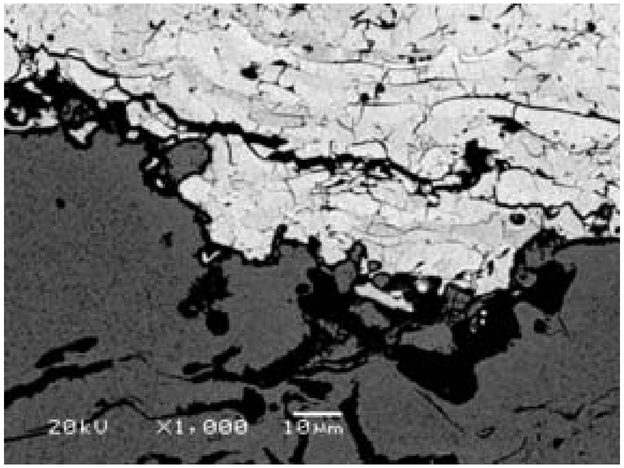

#6 $La_2Zr_2O_7$ and bond coat interface

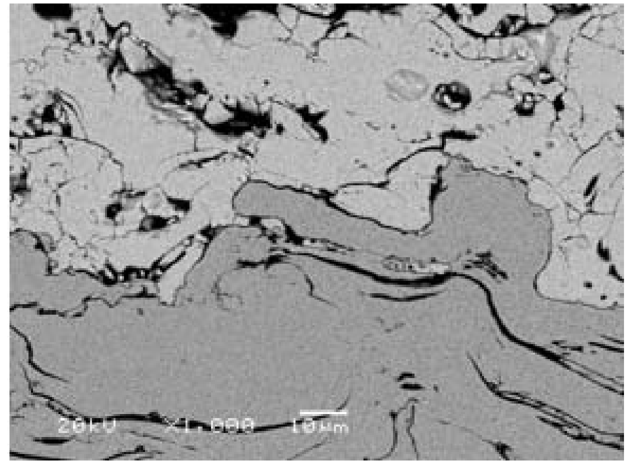

#7 porous 8YSZ and bond coat interface

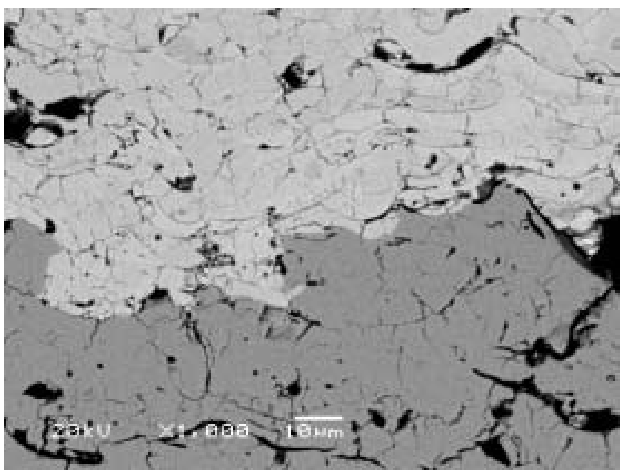

#8 $La_2Zr_2O_7$ and porous 8YSZ interface

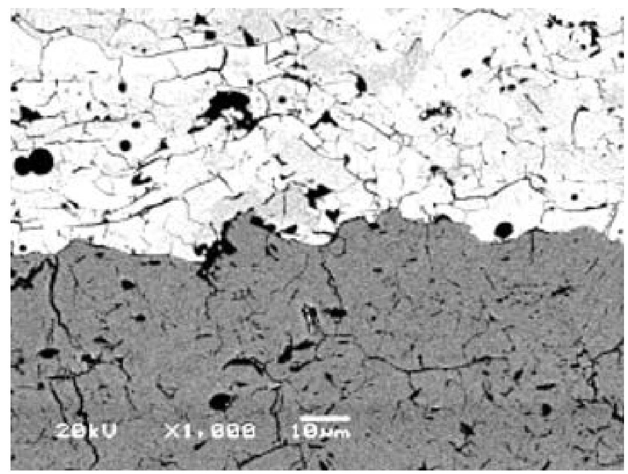

#9 $La_2Zr_2O_7$ and dense 8YSZ interface

Energy-dispersive X-ray spectroscopy

Applied heat treatments on sample #8

Heat treatment
1080℃ 4h
Ar atmosphere

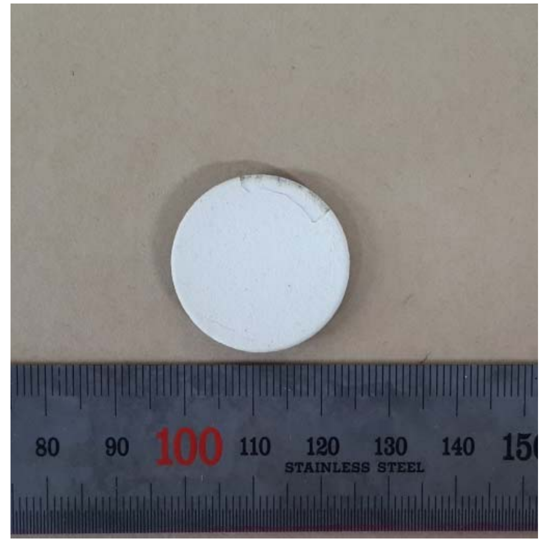

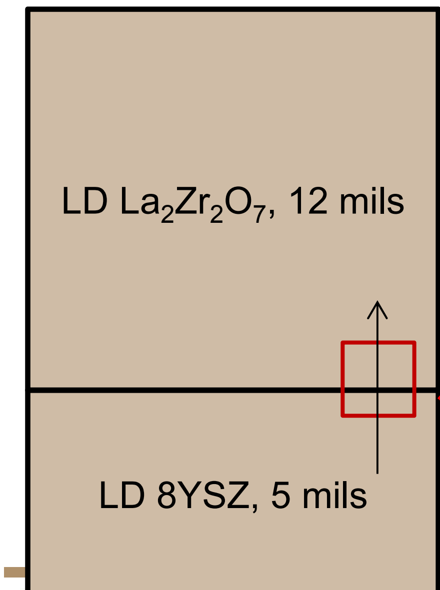

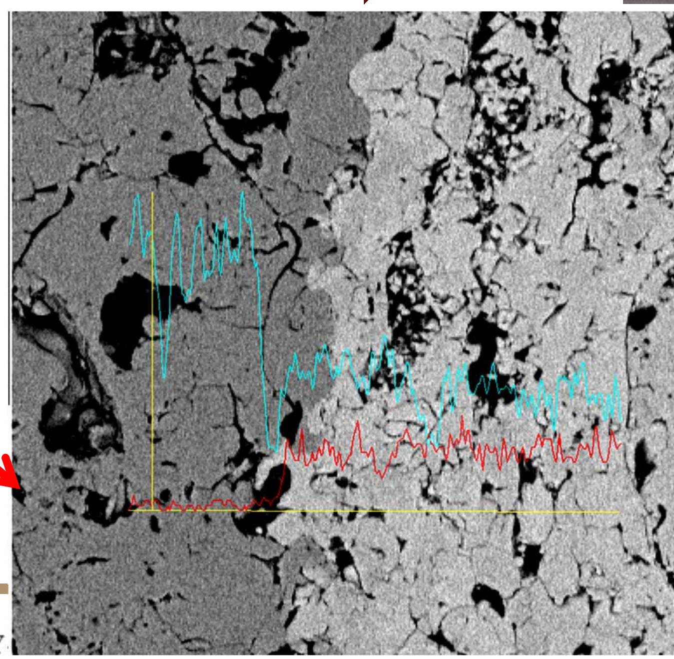

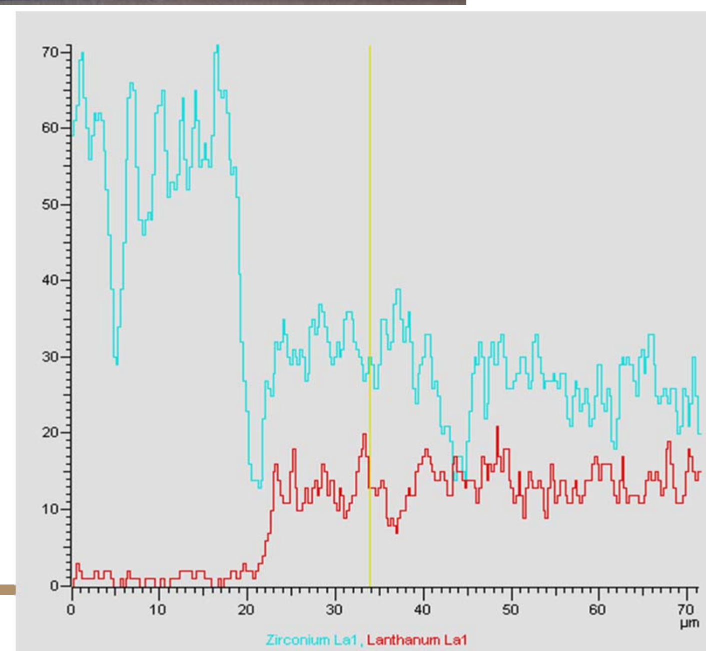

Vickers hardness of DCL

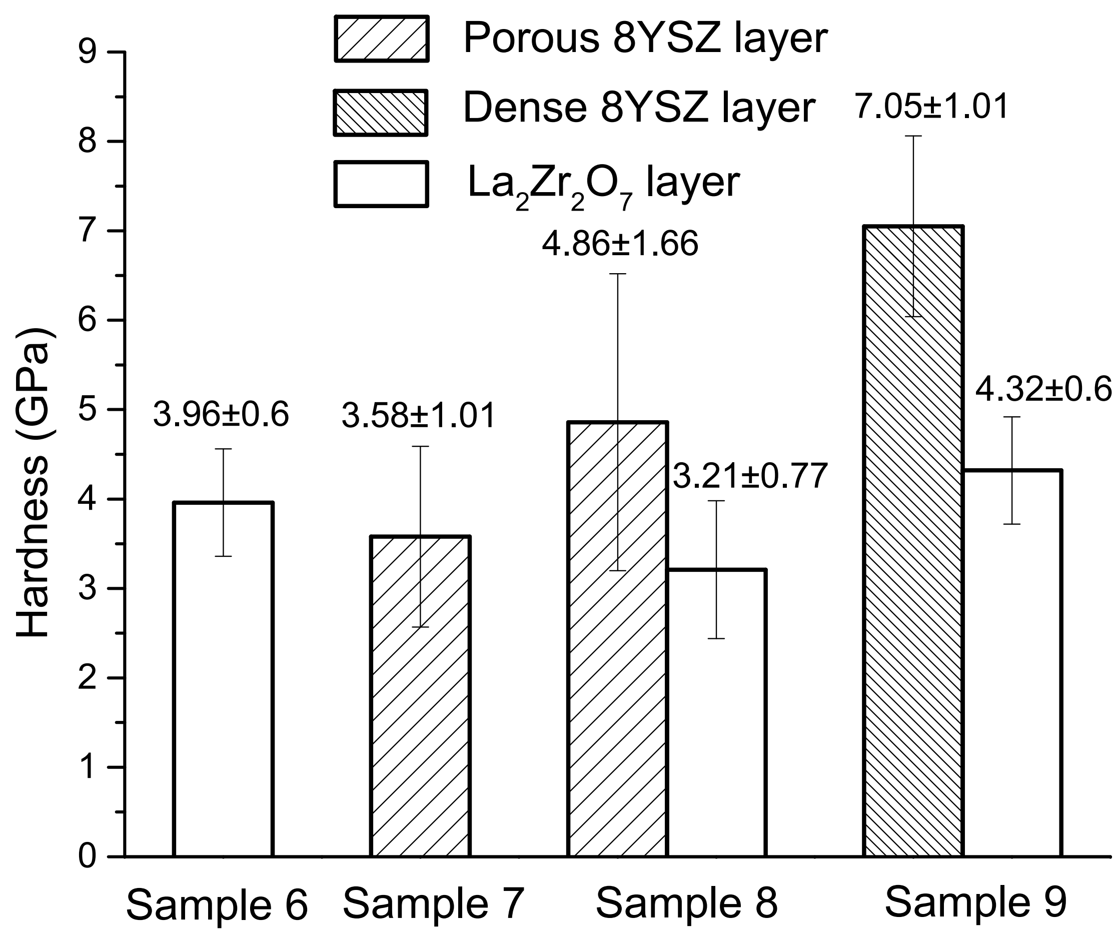

Bond strength test

Epoxy (FM 1000 adhesive film) to glue coating buttons to a mating cap.
Tensile test according to ASTM-C-633.

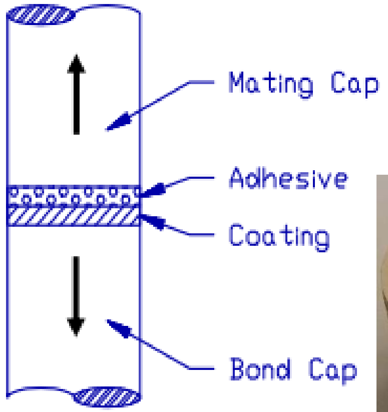

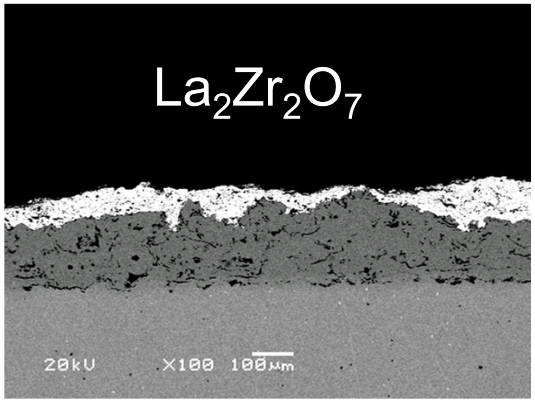

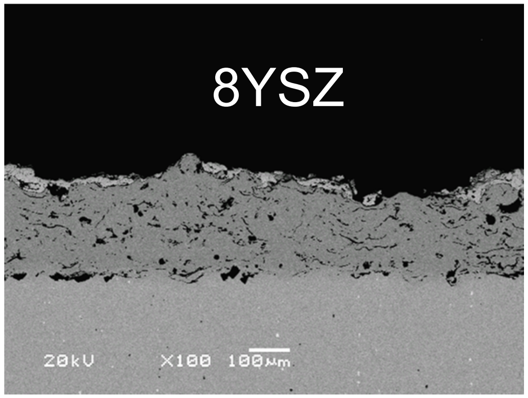

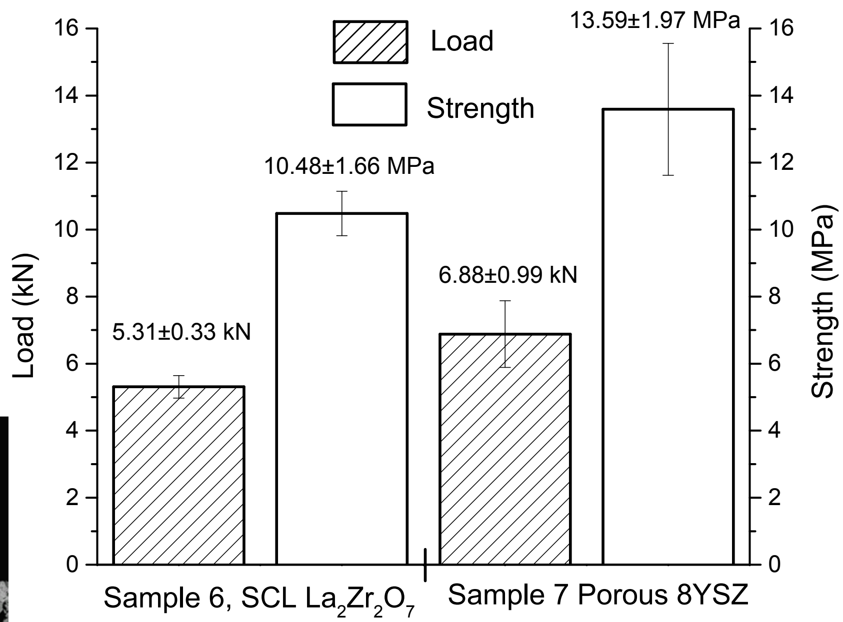

Residual stress distribution in coating

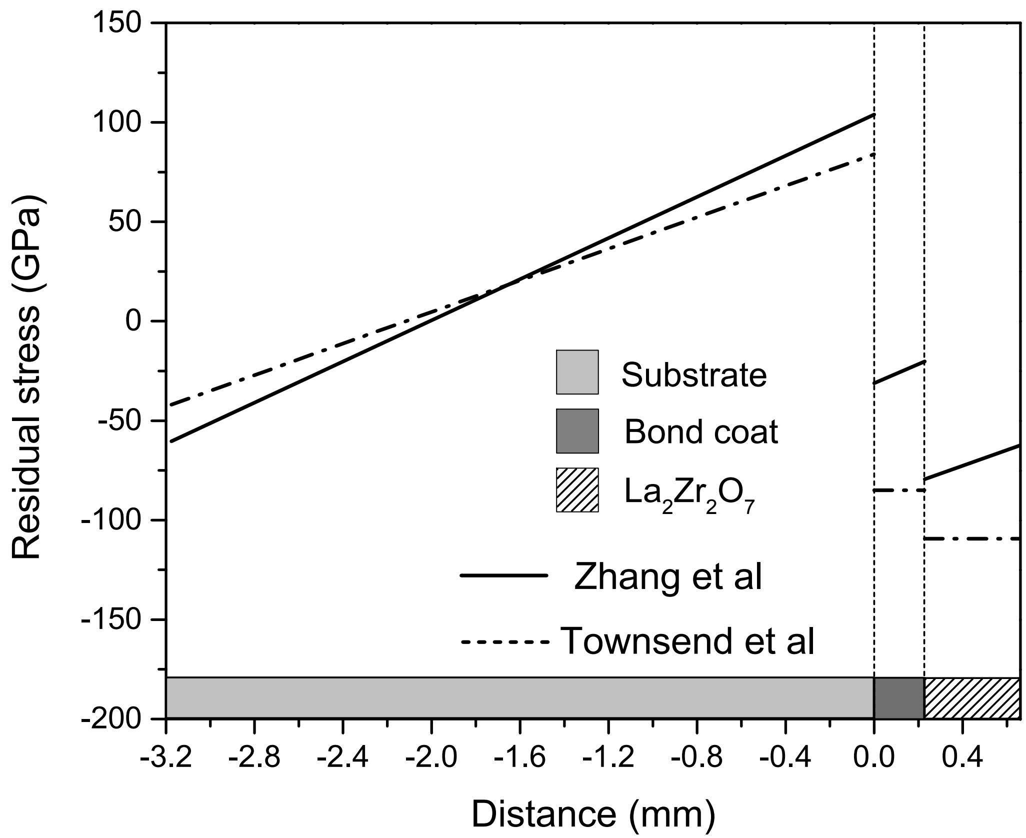

$$\sigma_s = E_s\left[\varepsilon_s + K\left(z+\delta\right)\right]$$

$$\sigma_i = E_i\left[\varepsilon_i + K\left(z+\delta\right)\right]$$

where $\varepsilon_i = \Delta\alpha\Delta T + \sum_{k=1}^{n}\frac{E_k t_k}{E_s t_s}(\alpha_k - \alpha_i)\Delta T$

$$\varepsilon_s = -\sum_{i=1}^{n}\frac{E_i t_i}{E_s t_s}\Delta\alpha\Delta T$$

$$\delta = \frac{t_s}{2} - \sum_{i=1}^{n}\frac{E_i t_i}{E_s t_s}\left(2h_{i-1} + t_i\right)$$

$$K = -\sum_{i=1}^{n}\frac{6E_i t_i \Delta\alpha\Delta T}{E_s t_s^{\,2}}$$

where α is the coefficient of thermal expansion (CTE), k is the ceramic coating layers range from 1 to n, t_i is the thickness of i^{th} layer.

X.C. Zhang, Thin Solid Films, 488 (2005) 274-282.

Erosion test

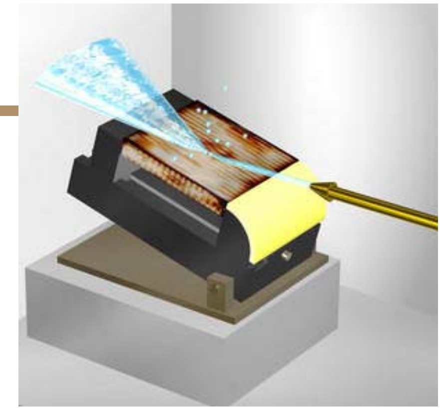

- 600±0.2g alumina sands with a diameter of 50 µm
- Spray rate 6 g/s; duration 100 s; spray angle 20°

#6, Single layer $La_2Zr_2O_7$ *#7, Porous 8YSZ.* *#8, $La_2Zr_2O_7$ +Porous 8YSZ* *#9, $La_2Zr_2O_7$ +Dense 8YSZ*

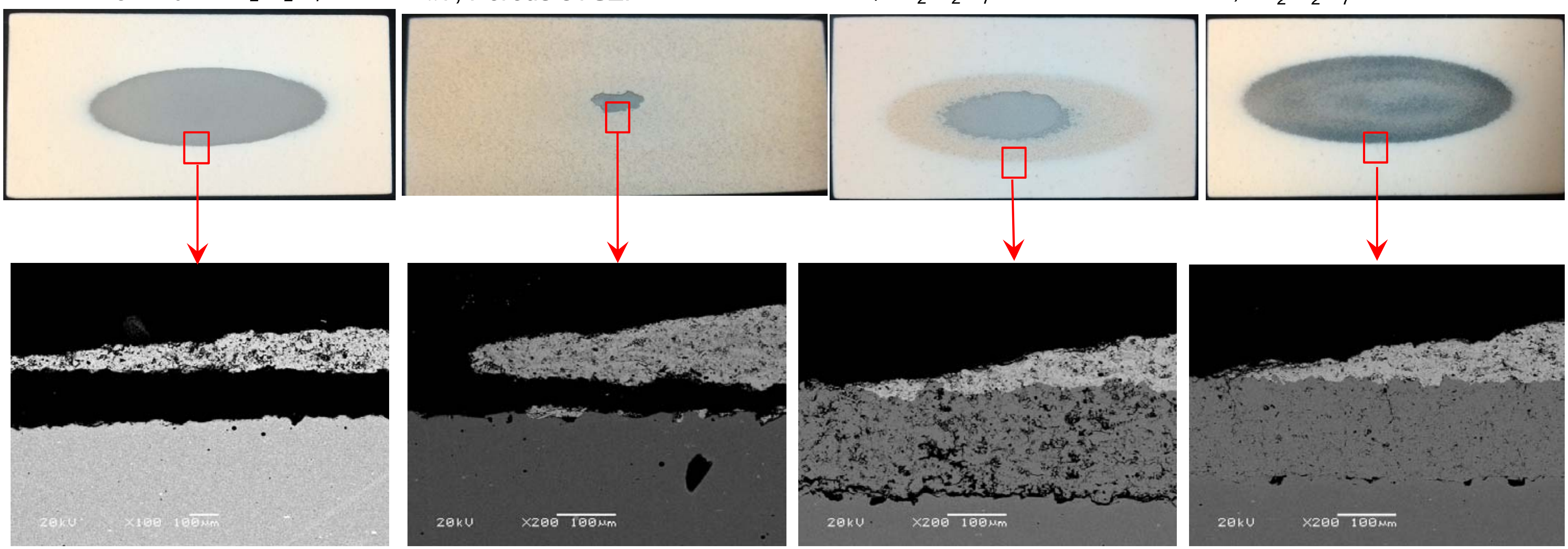

Erosion rate & critical erosion velocity

Erosion rate describes the erosion resistance of TBC sample [1]:

$$R_{erosion} = \frac{W_{removed\ material}}{W_{impacting\ particles}}$$

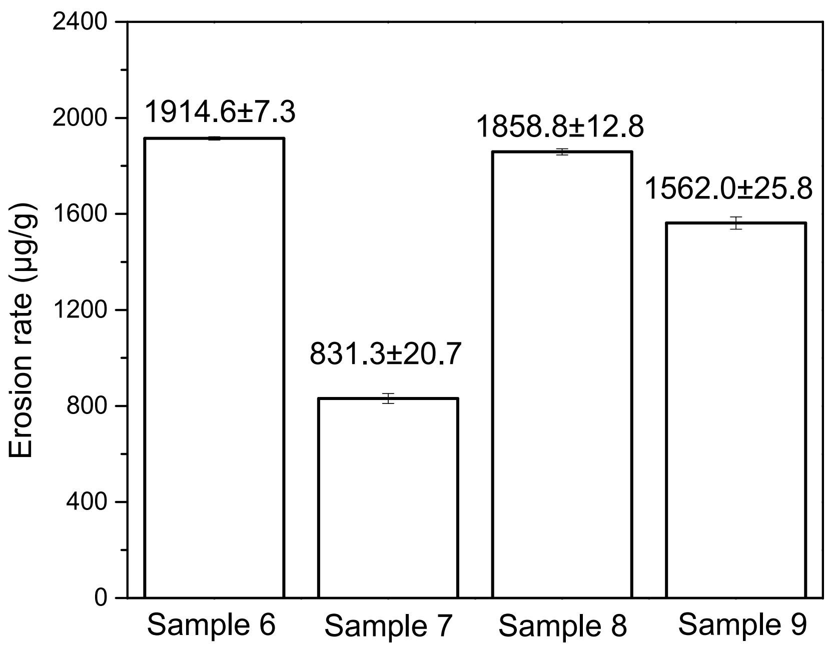

[1] D. Park, Int J Adv Manuf Technol, 23 (2004) 444-450.

Critical erosion velocity is used to express the critical condition to initiate cracks [2]:

$$V_{crit} = 105 \frac{E^{3/4} K_{IC}^{3}}{H^{13/4} \rho^{1/2} R^{3/2}}$$

E: Young's modulus
H: hardness
K_{IC} :fracture toughness
ρ: density of erodent particle
R: particle radius

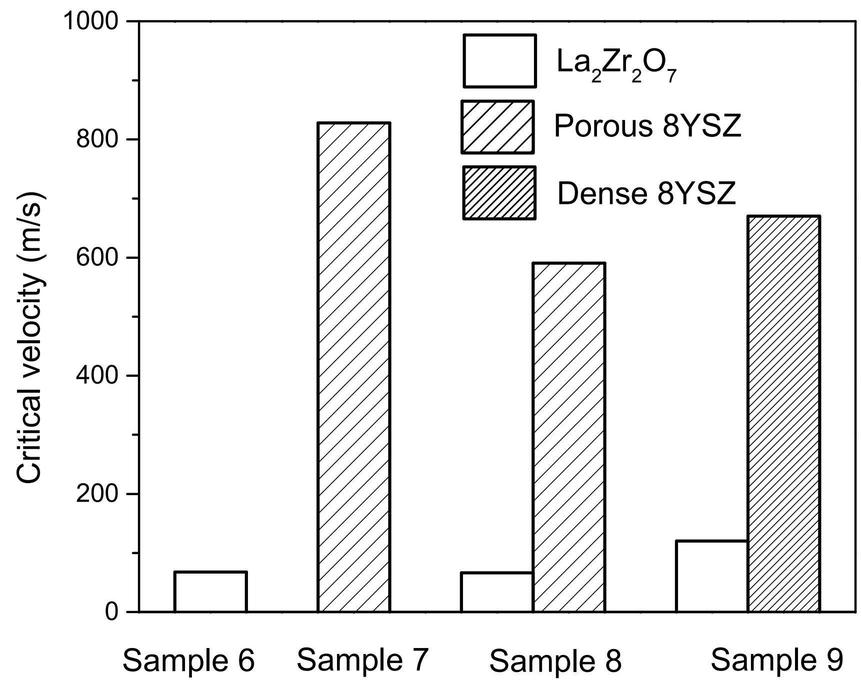

[2] R.G. Wellman, Wear, 256 (2004) 889-899.

Relationship between Vcrit and erosion rate

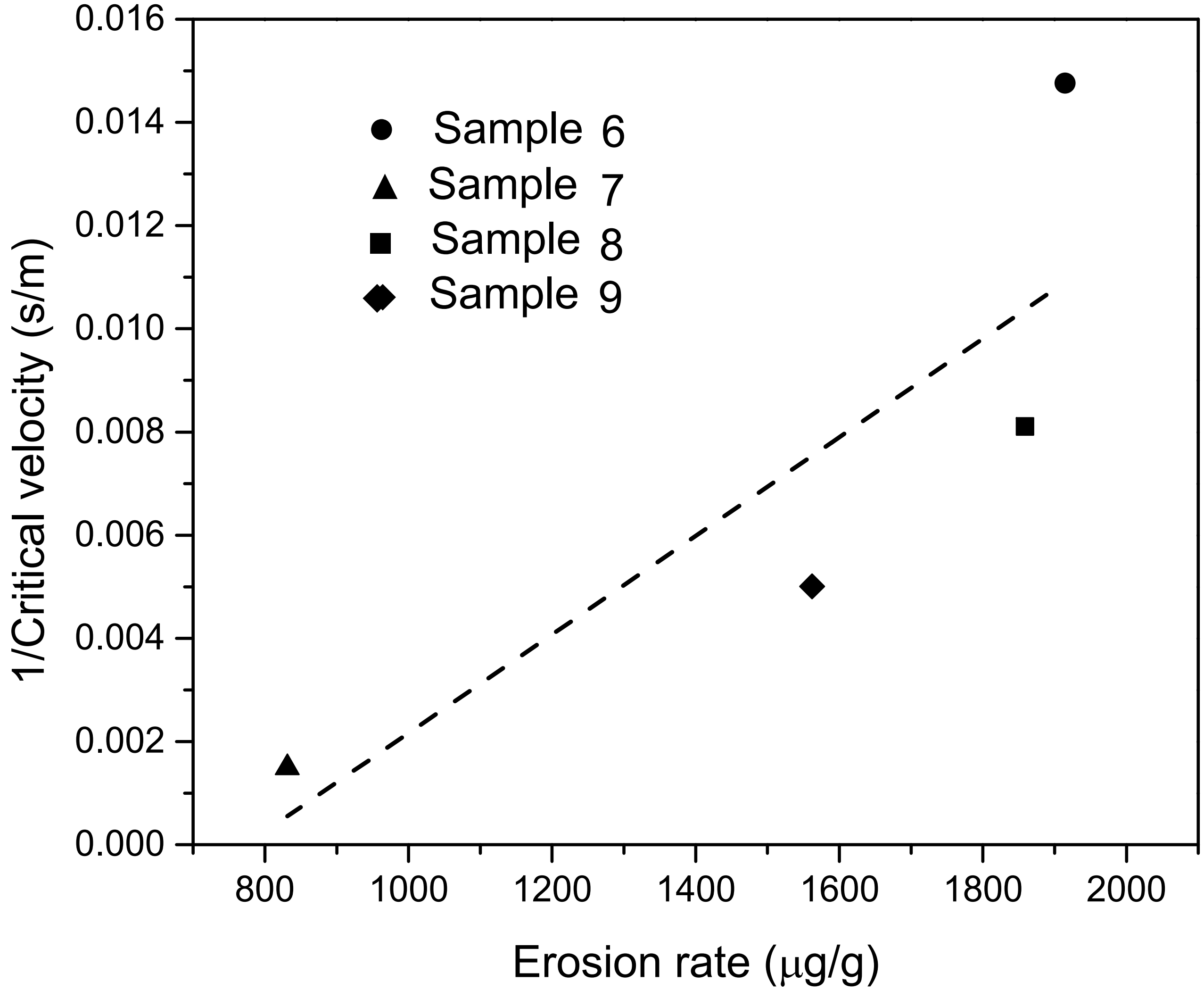

Outline

- Introduction
- Coating fabrications
- Single ceramic layer (SCL) architecture
- Double ceramic layer (DCL) architecture
- Characterization of physical and mechanical properties
- Microstructure and composition
- Porosity and hardness
- Bond strength test
- Erosion test
- Characterization of thermal properties
- Thermal properties
- Jet engine thermal shock tests
- Thermal gradient mechanical fatigue tests
- Summary and future work

Thermal conductivity

Thermal conductivity is determined from thermal diffusivity D_{th}, specific heat capacity C_p, and measured density ρ:

$$k = D_{th} \cdot C_p \cdot \rho$$

Thermal diffusivity is measured using laser flash diffusivity system (TA instrument DLF1200). Specific heat is measured by analytical method (TA instrument DLF1200)

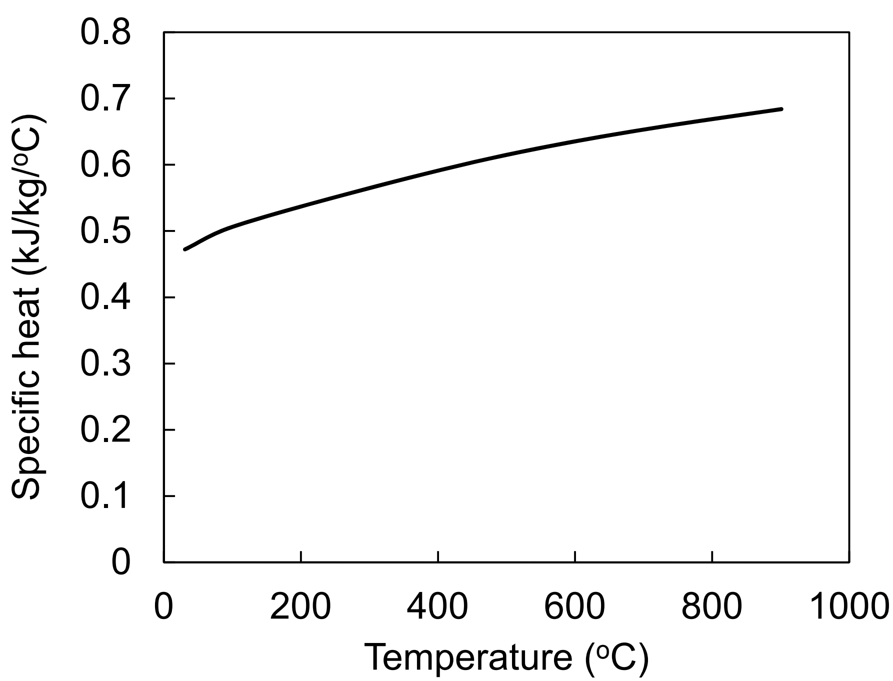

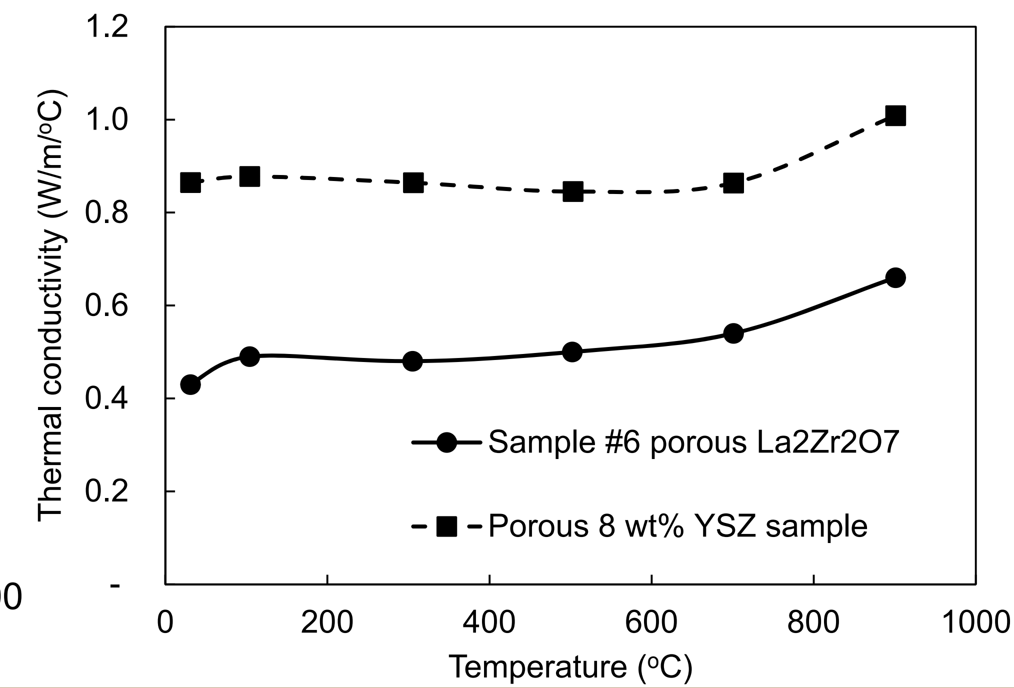

Thermal conductivity and heat capacity map

credit:
Jiangan Sun
@ ANL

TBC is 90.55% dense (ρ=5.478g/cc), with a nominal thickness of 600μm
Indentation marks are from previous study

Thermal conductivity and heat capacity map

Sample information

TBC:

Material: $La_2Zr_2O_7$

Thickness: ~600μm (this is used in calculation)

Density: 90.55% dense, dense density=6 g/cc, so density ρ = 5.478 g/cc

Specific heat: c = 0.54 J/g-K @1000C

Substrate (following are room temperature properties obtained from matweb):

Material: Haynes 188

Density: ρ = 8.98 g/cc

Thermal conductivity: k = 10.4 W/m-K,

Specific heat: c = 0.403 J/g-K, (therefore, ρc = 3.62 J/cm^3-K)

Thickness used in calculation: L = 4 mm (may have a small effect to results)

Test condition

Flash thermal imaging test with one flash lamp

Imaging speed: 994 Hz; imaging duration: 3 seconds

Measured TBC thermal properties

Thermal conductivity *k* image

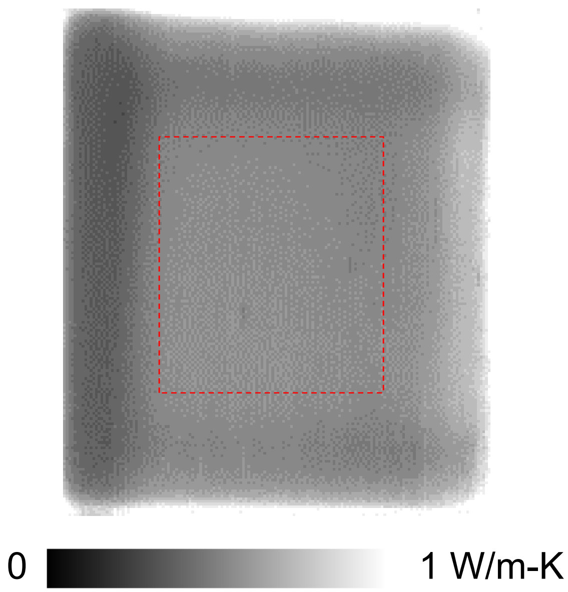

Heat capacity ρc image

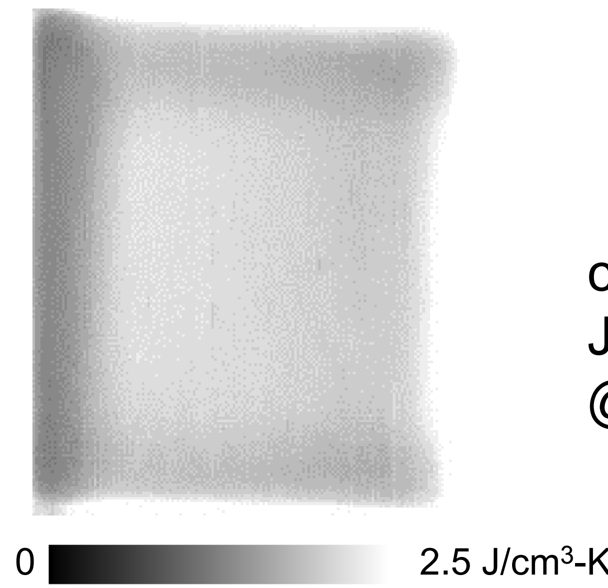

credit:
Jiangan Sun
@ ANL

Predicted average TBC properties (within red rectangular area):

k = 0.55 W/m-K, ρc = 2.16 J/cm^3-K

- These results were based on a TBC thickness of 600 μm
- TBC specific heat @RT: c = 0.393 J/g-K; predicted TBC density is: $\rho = \rho c/c = 2.16/0.393 = 5.5$ g/cc

Coefficient of thermal expansion (CTE)

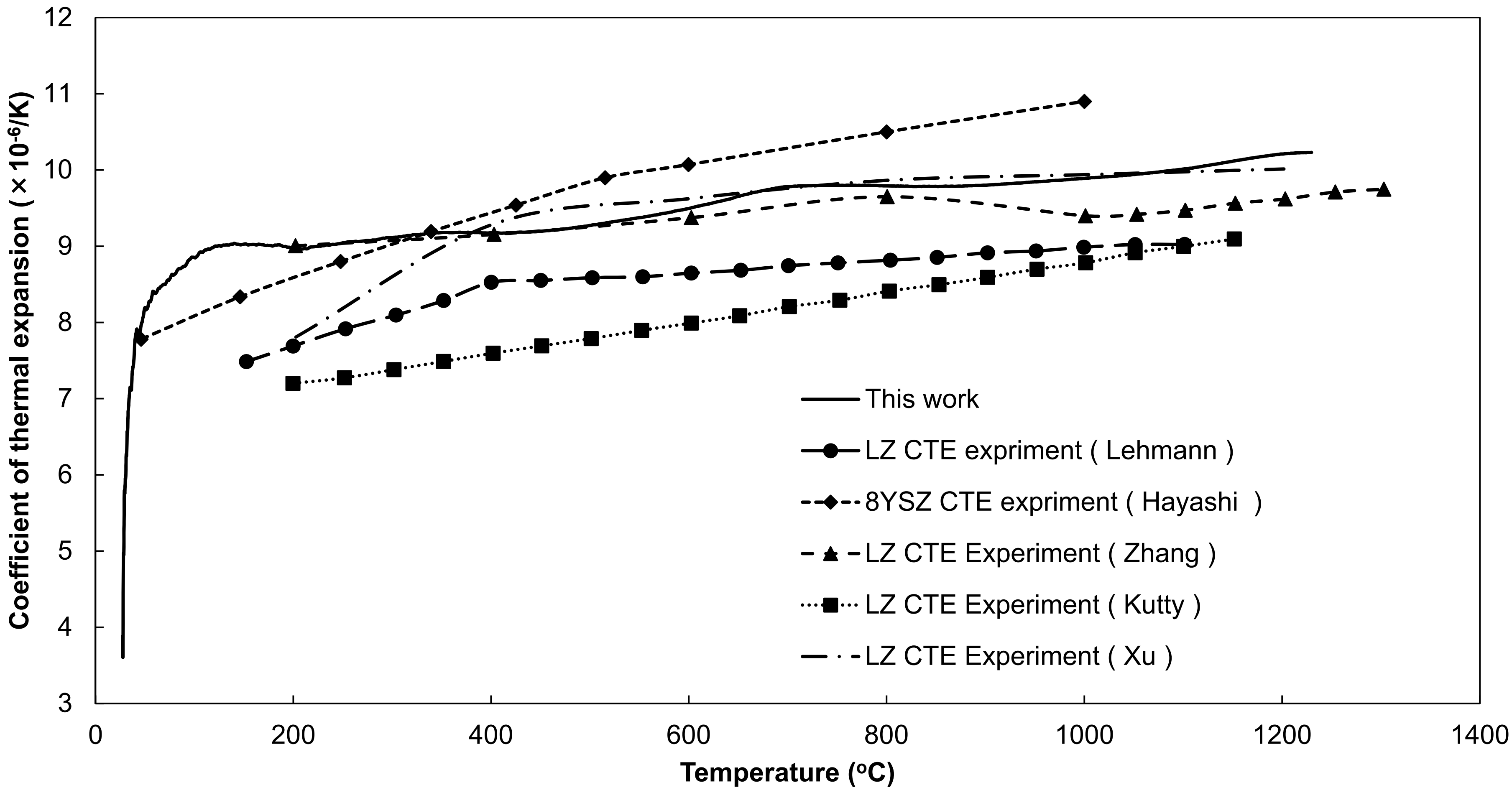

CTE is measured using a BAEHR dilatometer from 25 to 1400 °C.

H. Lehmann, D. Pitzer, G. Pracht, R. Vassen, D. Stöver, Journal of the American Ceramic Society, 86 (2003) 1338-1344.
H. Hayashi, T. Saitou, N. Maruyama, H. Inaba, K. Kawamura, M. Mori, Solid State Ionics, 176 (2005) 613-619.
J. Zhang, J. Yu, X. Cheng, S. Hou, Journal of Alloys and Compounds, 525 (2012) 78-81.
K.V.G. Kutty, S. Rajagopalan, C.K. Mathews, U.V. Varadaraju, Materials Research Bulletin, 29 (1994) 759-766
C. Xu, C. Wang, C. Chan, K. Ho, Physical Review B, 43 (1991) 5024-5027.

Jet engine thermal shock tests (JETS)

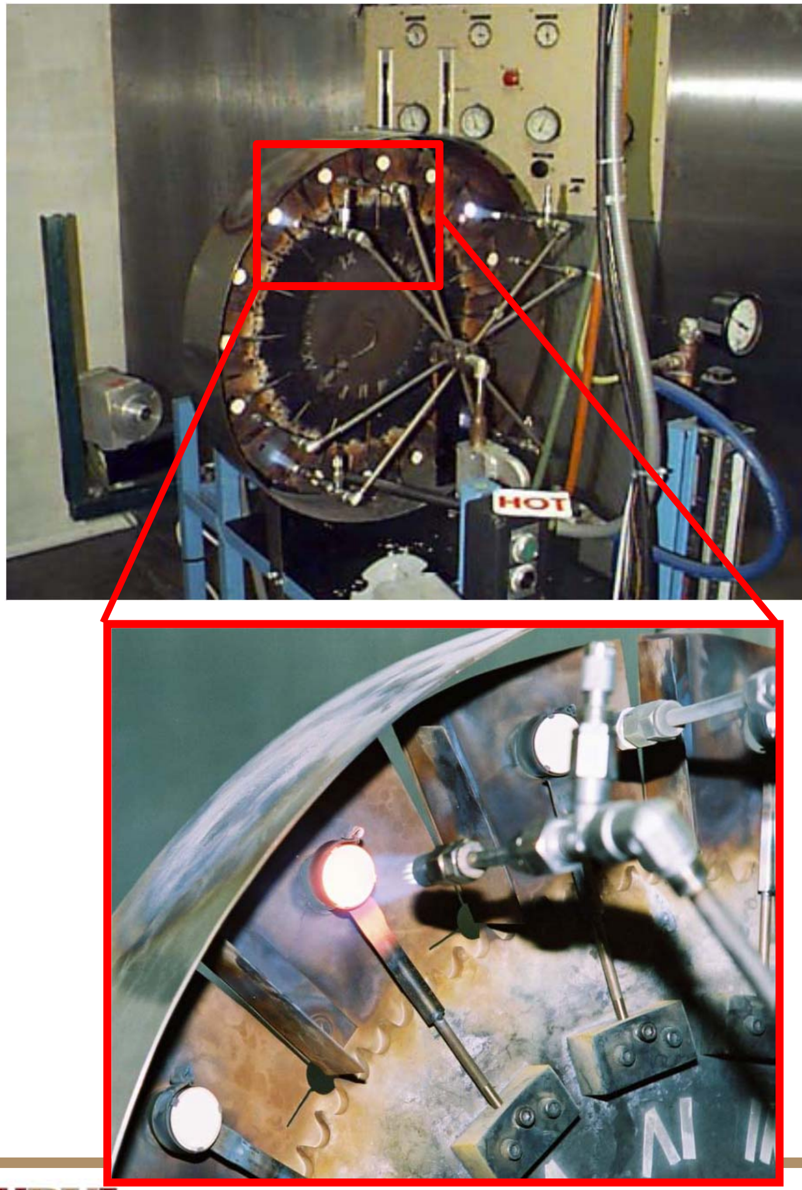

- Jet engine thermal shock (JETS) tests are conducted to investigate the thermal cycling performance.
- TBC samples are heated to 2250 °F (1232.2 °C) at the center for 20 s, and then cooled by compressed N_2 cooling for 20 s, and then ambient cooling for 40 s.
- Temperatures are measured by thermal couple and pyrometer.

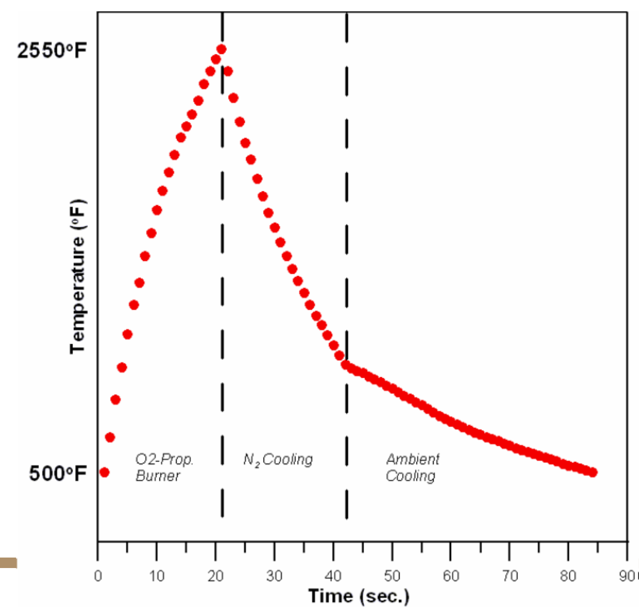

Jet engine thermal shock test (JETS) results

#6, Single layer $La_2Zr_2O_7$

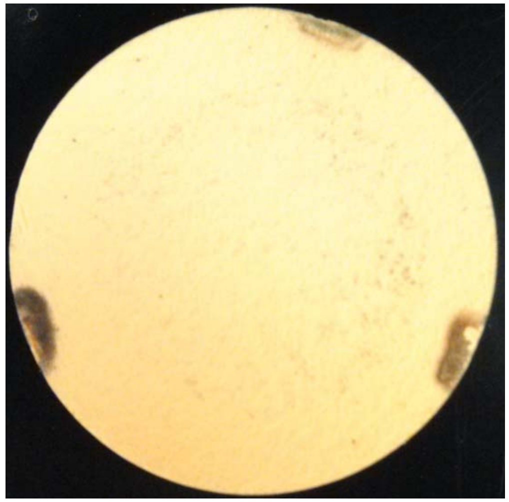

#7, Porous 8YSZ

#8, Porous 8YSZ+ $La_2Zr_2O_7$

#9, Dense 8YSZ+ $La_2Zr_2O_7$

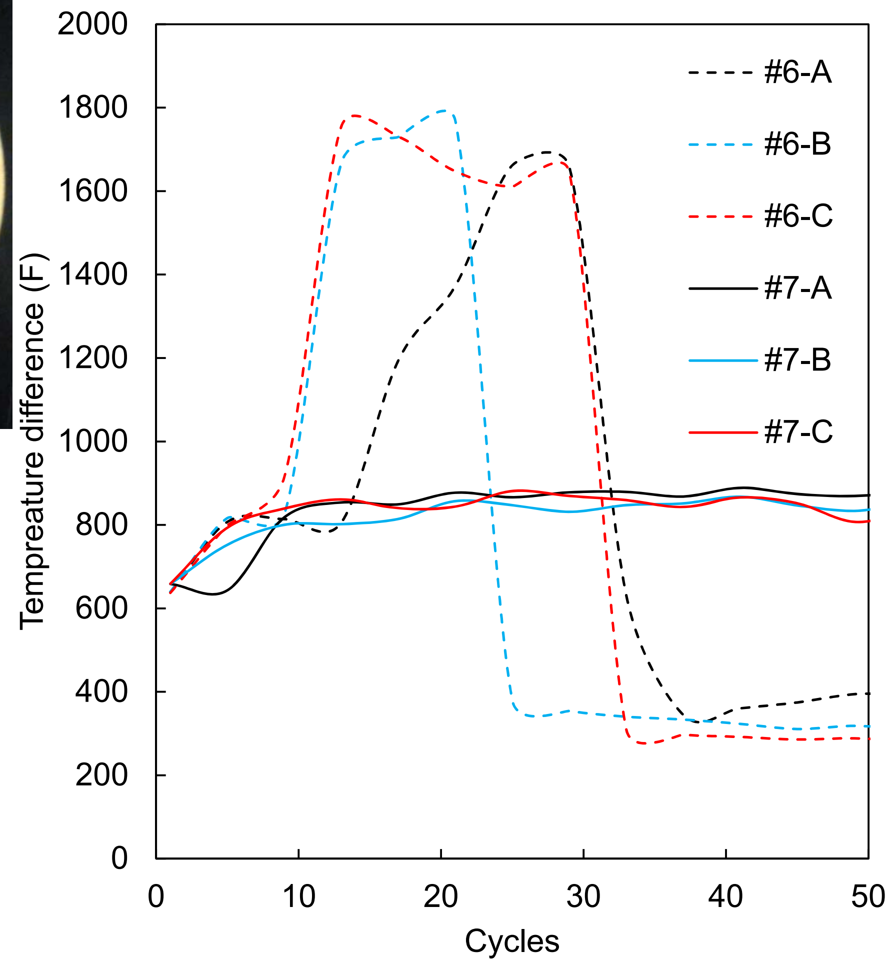

Thermal gradient mechanical fatigue (TGMF)

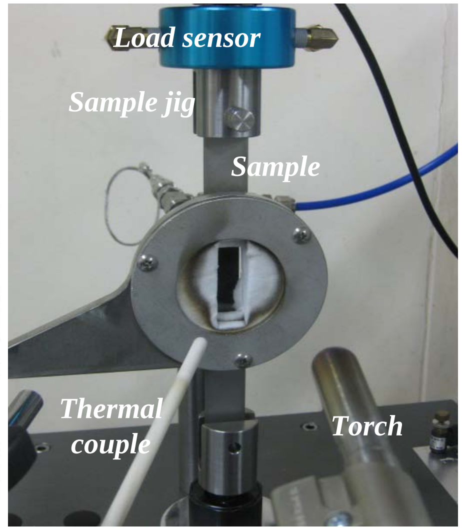

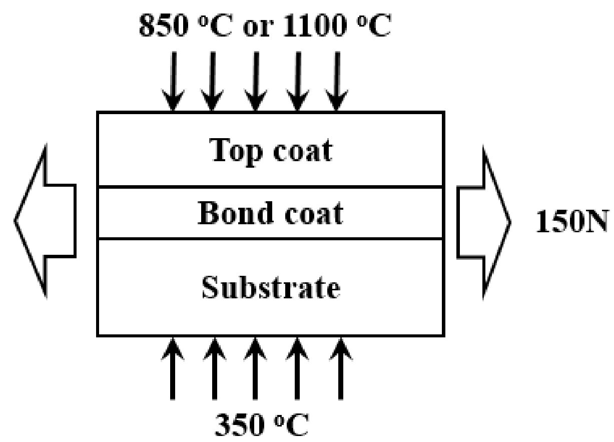

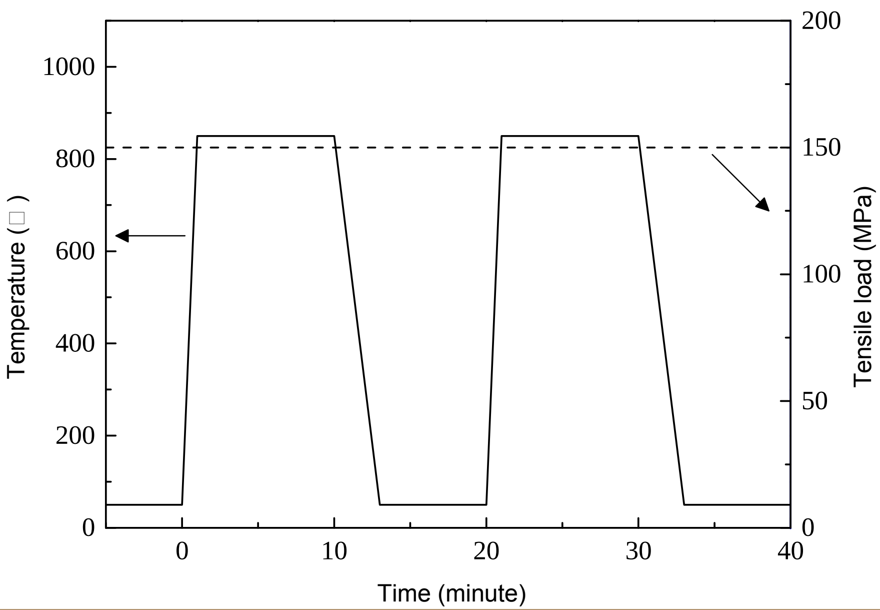

At 850 °C

Sample	Test cycle
SCL porous 8YSZ	1200
DCL porous 8YSZ + $La_2Zr_2O_7$	220
DCL dense 8YSZ + $La_2Zr_2O_7$	50

At 1100 °C

Sample	Test cycle
DCL porous 8YSZ + $La_2Zr_2O_7$	38
DCL dense 8YSZ + $La_2Zr_2O_7$	49

$La_2Zr_2O_7$ thermal conductivity calculation

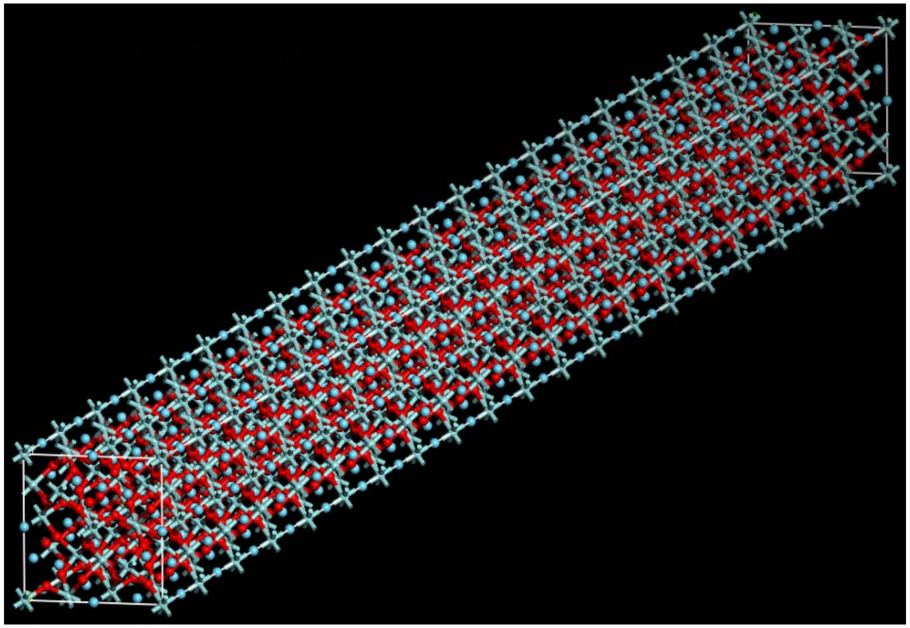

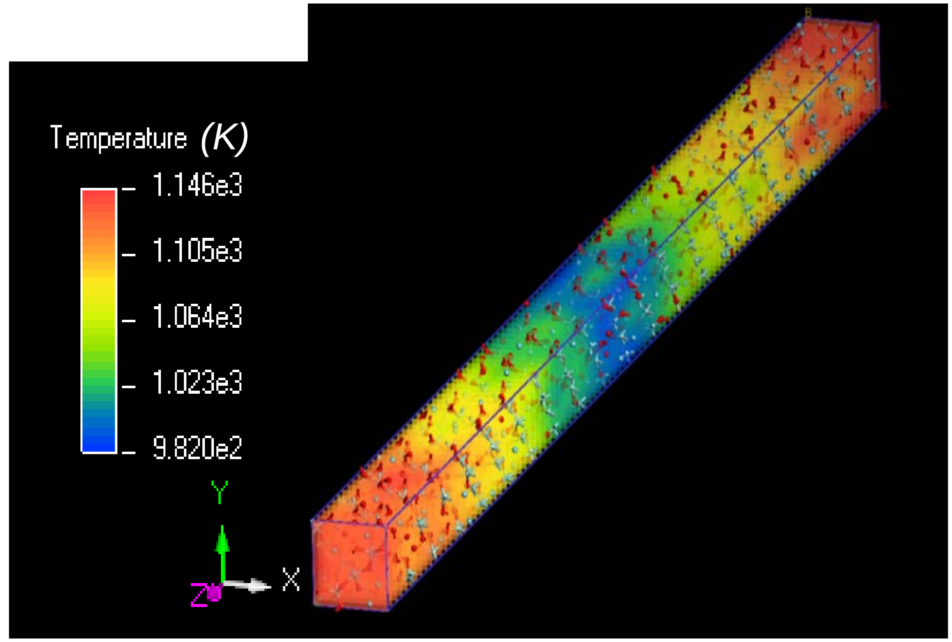

Replicate 20 conventional cells along the heat flow direction to form a super cell

Calculated temperature contour based on Fourier's law $k = -\overrightarrow{q''}/\vec{\nabla}T$

The calculated thermal conductivity is 1.2 W/m/K at the temperature of 1000 ^{o}C, which is reasonably in agreement with the experimentally measured thermal conductivity ~1.5 W/m/K [1].

[1] R. Vassen, X. Cao, F. Tietz, J. Am. Ceram. Soc., 83 (2000) 2023–2028.

Imaged based FEM calculation of thermal conductivity of $La_2Zr_2O_7$ TBC

SEM image **Binary image** **FEM model**

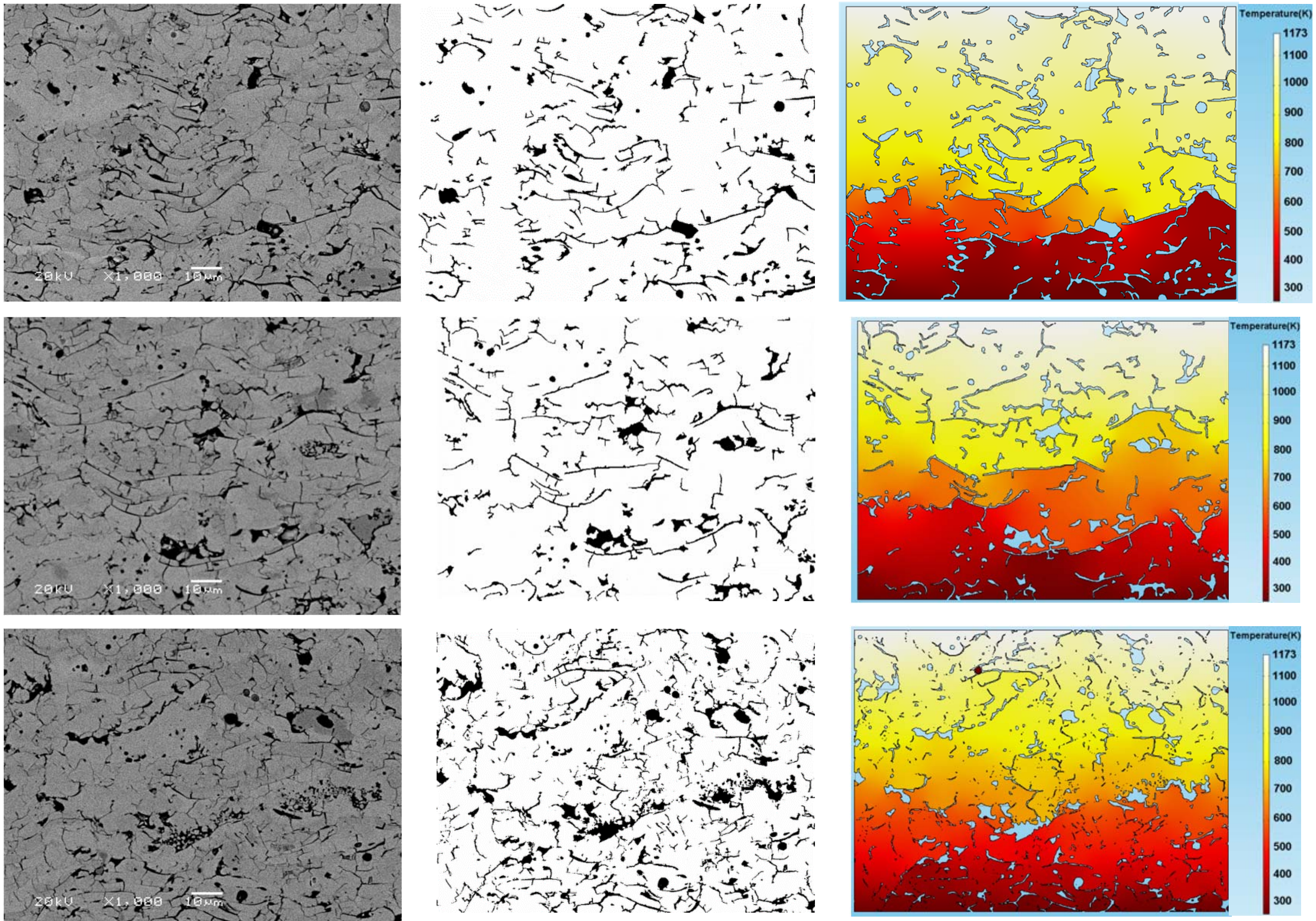

k=0.538 W/m/K

k=0.550 W/m/K

k=0.723 W/m/K

Thermal conductivity of fully dense LZ *k*=1.5 W/m/K

Imaged based FEM calculation of thermal conductivity of $La_2Zr_2O_7$ coating

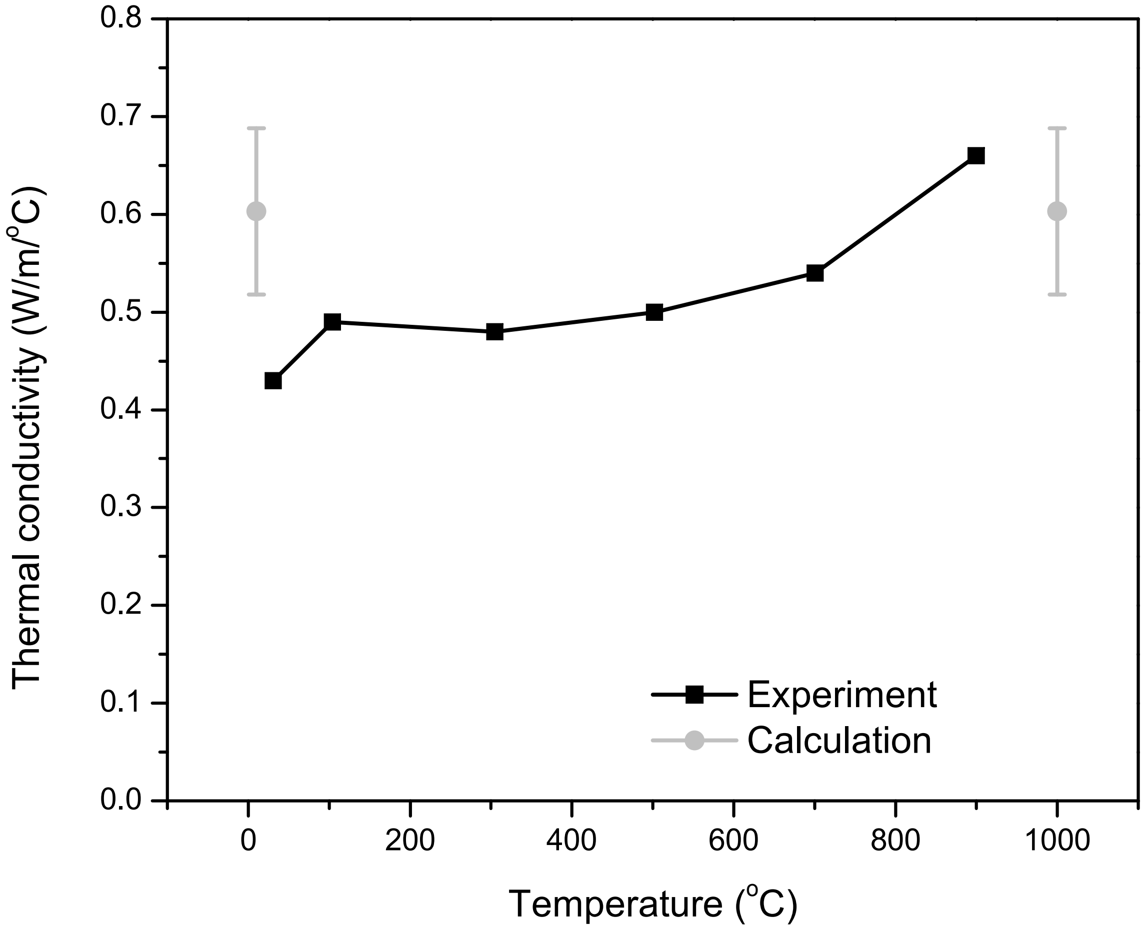

Calculated thermal conductivity 0.60±0.08 W/m-K, in good agreement with experimental data.

Summary

- $La_2Zr_2O_7$ powder, coating microstructure and chemistry characterizations show that $La_2Zr_2O_7$ is stable at high temperatures, which makes it suitable for TBC applications.
- Mechanical properties (hardness, bond strength) are similar to 8YSZ.
- Thermal conductivity of $La_2Zr_2O_7$ is lower than 8YSZ of similar porosity.
- Thermal properties using *ab initio* and image-based finite element model calculations are in good agreement with experiments.

Future work

- Thermal cycling behavior of $La_2Zr_2O_7$ needs to be improved.

Composite coatings with buffer layers

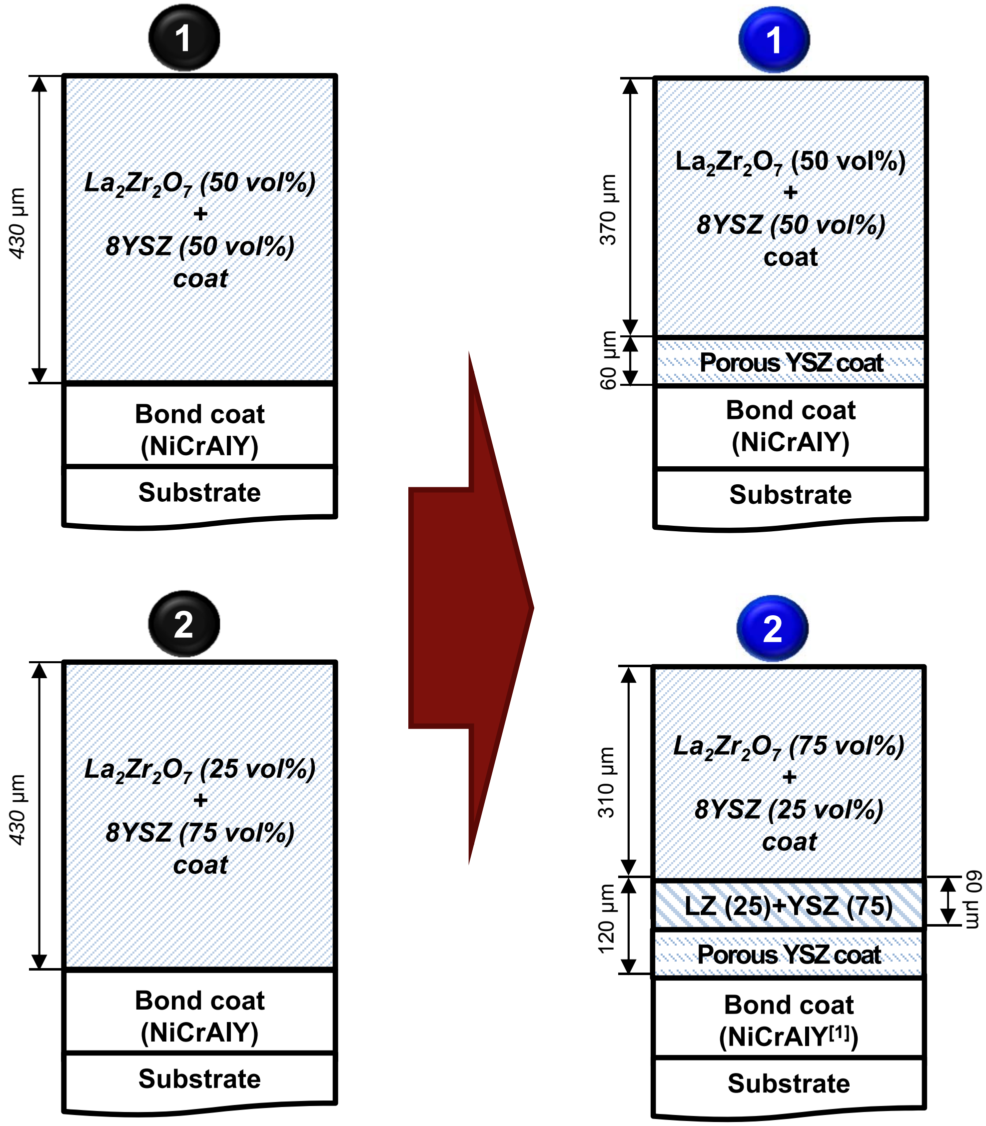

Composite top coats:

thermal conductivity + matching CTEs

Introducing buffer layer:

Increasing strain compliance + Decreasing CTEs mismatch

2nd buffer layer:

Further decrease CTEs mismatch

Publications and presentations

1. Jing Zhang, Yeon-Gil Jung, Li Li, co-organize "**Advanced Coating Materials for Energy and Environmental Applications**" **symposium in Materials Science & Technology 2015 (MS&T15), October 4-8, 2015, Columbus, OH**
2. Jing Zhang, Yeon-Gil Jung (eds.), 1st International Joint Mini-Symposium on Advanced Coatings, Materials Today: Proceedings, 2014
3. Yeon-Gil Jung, Zhe Lu, Ungyu Paik, and Jing Zhang, Lifetime Performance of Thermal Barrier Coatings in Thermally Graded Mechanical Fatigue Environments, The 11th International Conference of Pacific Rim Ceramic Societies(PacRim-11), Jeju, Korea, August 30 - September 4, 2015
4. Yeon-Gil Jung, Zhe Lu, Qi-Zheng Cui, Sang-Won Myoung, and Jing Zhang, Thermal Durability and Fracture Behavior of Thermal Barrier Coatings in Thermally Graded Mechanical Fatigue Environments, the International Symposium on Green Manufacturing and Applications 2015 (ISGMA 2015), Qingdao, China, June 23 - June 27, 2015
5. Xingye Guo, Jing Zhang, Zhe Lu, Yeon-Gil Jung, Theoretical prediction of thermal and mechanical properties of lanthanum zirconate nanocrystal, the 1st International Conference & Exhibition for Nanopia, Changwon Exhibition Convention Center, Gyeongsangnam-do Province, Miryang City, Korea, November 13-14, 2014
6. Sang-Won Myoung, Zhe Lu, Qizheng Cui, Je-Hyun Lee, Yeon-Gil Jung, Jing Zhang, Thermomechanical properties of thermal barrier coatings with microstructure design in cyclic thermal exposure, the 1st International Conference & Exhibition for Nanopia, Changwon Exhibition Convention Center, Gyeongsangnam-do Province, Miryang City, Korea, November 13-14, 2014
7. Zhang, J., X. Guo, Y.-G. Jung, L. Li, and J. Knapp, Microstructural Non-uniformity and Mechanical Property of Air Plasma-sprayed Dense Lanthanum Zirconate Thermal Barrier Coating. Materials Today: Proceedings, 2014. 1(1): p. 11-16.
8. Guo, X. and J. Zhang, First Principles Study of Thermodynamic Properties of Lanthanum Zirconate. Materials Today: Proceedings, 2014. 1(1): p. 25-34.